Supporting Information

Chemisorbed Oxygen or Surface Oxides Steer the Selectivity in Pd Electrocatalytic Propene Oxidation Observed by Operando Pd L-edge X-ray Absorption Spectroscopy

Sergey Koroidov,[*a] Anna Winiwarter,[†b] Oscar Diaz-Morales, [†a] Mikaela Görlin,[†a] Joakim Halldin Stenlid,[†a] Hsin-Yi Wang,[a] Mia Börner,[a] Christopher Goodwin,[a] Markus Soldemo,[a] Lars Gunnar Moody Pettersson,[a] Jan Rossmeisl,[c] Tony Hansson,[a] Ib Chorkendorff,[b] and Anders Nilsson,[*a]

Chemicals and materials

All chemicals were purchased in analytical grade quality and used as received. Conductive graphene sheets (substrates) were purchased form Graphene Supermarket, Graphene Laboratories Inc.

Nitrogen and Helium (grade N5, Airgas, USA)

Propene (grade 3N5, Advanced Specialty Gases, NV, USA)

The electrolyte was prepared by partially neutralizing a 0.1 M H_3PO_4 solution with 2.5 M NaOH (≥99.996 %, metals basis, Alfa Aesar) to reach pH 2.83. The dilute acid and base were prepared from concentrated H_3PO_4 (≥85 wt. % in H_2O, Sigma-Aldrich) and NaOH (≥98%, Sigma-Aldrich) by dilution with ultra-pure water (Milli-Q, 18 MΩ cm).

Electrocatalyst preparation

Working electrodes were prepared by DC sputtering of Pd at 5 mTorr Ar pressure and 20 W onto the as-received substrates. The sputtering rate was estimated by QCM and the amount of deposited Pd to a film thickess of 5 nm.

Electrocatalyst characterization

The morphology and composition of the palladium films was assessed by ex-situ scanning electron microscopy (SEM) and X-ray photoemission spectroscopy (XPS).

SEM

Scanning electron microscopy images were recorded using a JOEL JSM-7000F with field emission gun. SEM images were recorded in high vacuum mode, with 5 kV acceleration voltage.

(A) As prepared (B) After oxidation in N_2 (C) After oxidation in propene

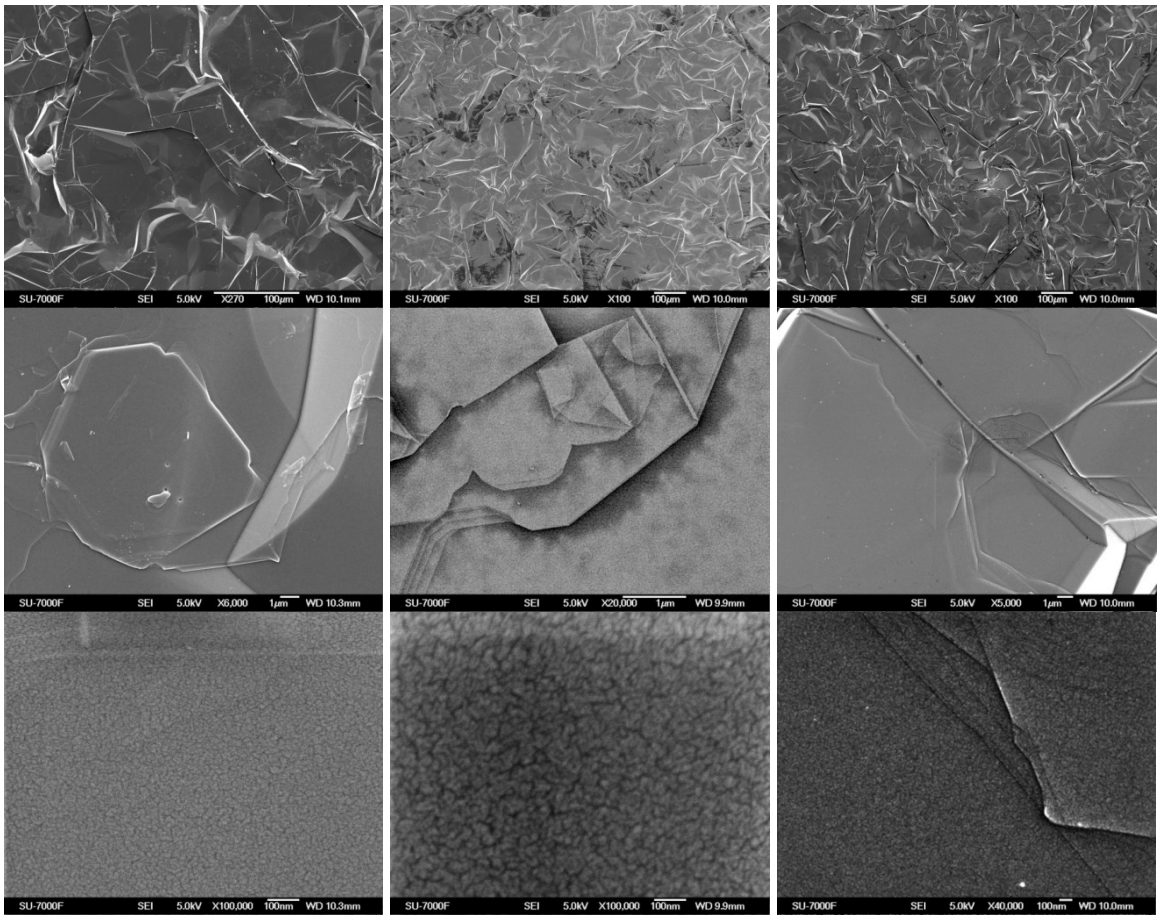

Figure S1. SEM images of Pd electrocatalysts on conductive graphene sheet A) as sputtered Pd film; B) Pd film after electrochemical oxidation in N_2 saturated electrolyte (0.1 M phosphate buffer pH 2.83) at 1.3 V vs RHE for 50 min C) after electrochemical oxidation in propene saturated electrolyte at 1.3 V vs RHE for 50 min. A pre-adsorption step was carried out at 0.68 V vs. RHE for 15 min in either propene or N_2 saturated electrolytes. We observe that electrochemical oxidation in N_2 affects the catalyst nanostructure more significantly than propene, and leads to an increase in the particle sizes of Pd after the reaction. The change in particle size observed after oxidation in N_2 agrees with formation of a surface layer such as an oxide, which is only seen on the largest magnification. After both electrochemical measurements B) and C) original structure is still present in a lowest magnification.

X-ray photoelectron spectroscopy (XPS)

The XPS measurement of the prepared electrode was carried out with ThermoScientific Thetaprobe instrument equipped with an Al Kα X-ray source. The chamber base pressure was approximately $1x10^{-7}$ mbar, an Ar flood gun was used for charge neutralisation of the samples. For survey spectra, 20 scans were recorded with 50 ms dwell time per 1 eV step, pass energy 100 eV. The use of multiple scans permits identification of potential charging effects between scans.

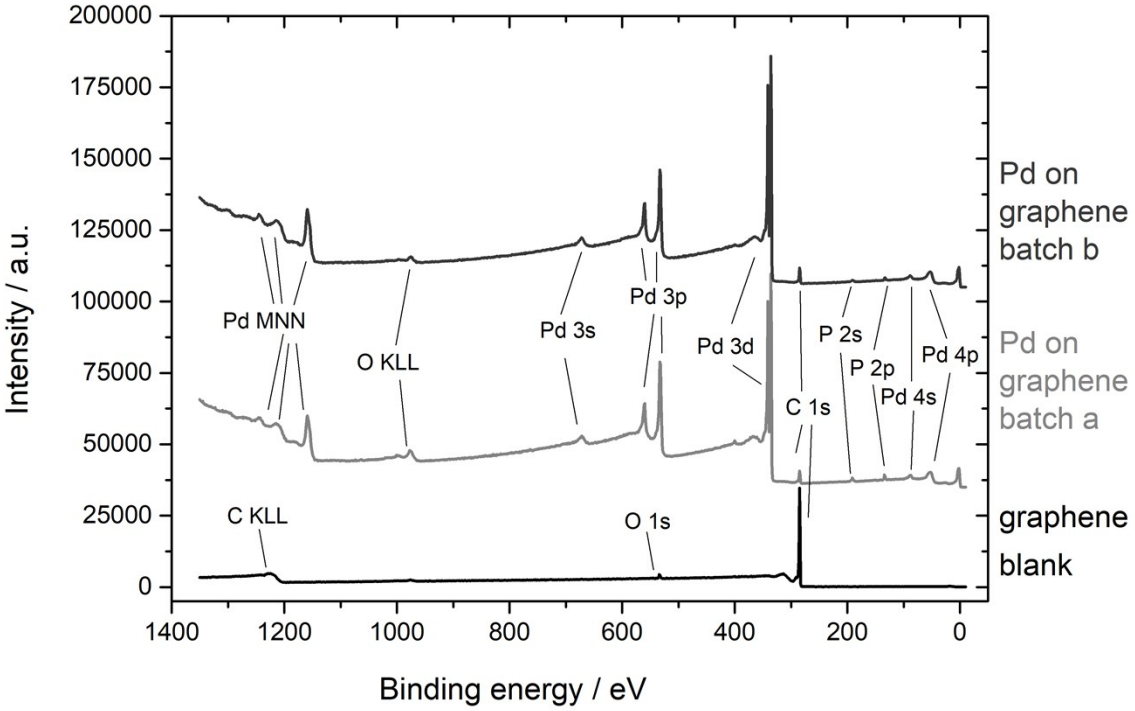

Figure S2: XPS spectra of Pd electrocatalyst on conductive graphene sheet (black) and conductive graphene sheet of two batches used for the experiments (grey). Common core-level peaks and Auger electron peaks are indicated. The spectra are offset in intensity for clarity.

Characterization of reference samples by Hard X-ray photoelectron spectroscopy (HAXPES)

Hard X-ray photoelectron spectroscopy measurements on a single crystal Pd(100) sample were performed as reference measurements of the Pd $2p_{3/2}$ core-electron binding energy. The measurements were carried out on both oxidized and reduced Pd(100) surface. The measurements were carried out using the POLARIS endstation at the P22 beamline at PETRA III, DESY, Germany.[1] The beamline provided photons of energy 4600 eV, the binding energy scale was calibrated to the Fermi edge. The POLARIS endstation is equipped with a modified ScientaOmicron HiPP-2 electron analyzer and the incidence light comes at an angle of 89.7° off the surface normal vector (high grazing incidence), meaning extremely surface sensitive. The spectra were collected with a pass energy of 200 eV, 1 sweep, 50 meV steps, and 0.257 s dwell time. Spectra were collected for an oxidized surface (PdO) and a reduced surface that partly was oxidized, see Figure S3. Both spectra have been normalized to the Pd oxide peak to amplify structural differences. The binding energies of the PdO peak and the metallic Pd peak were determined by peak fitting. The metallic peak, $Pd^0_{3/2}$, was fitted by first removing the Pd oxide signal by subtraction with the PdO signal and then using a Voigt function to fit the remaining signal. It is found that the PdO peak is shifted 1.6 eV towards higher binding energies compared to the metallic peak. This result is in close agreement with literature values. [2]

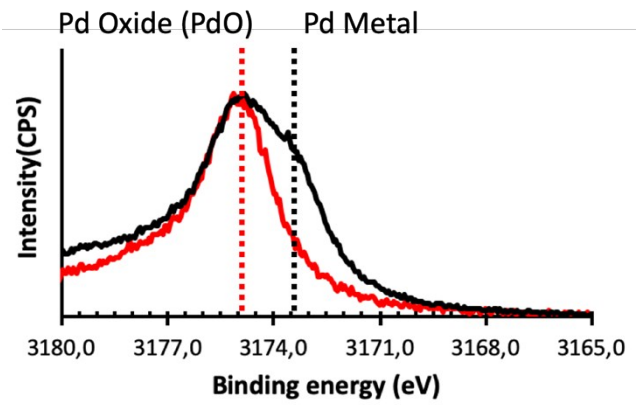

Figure S3: XPS spectra showing the peak positions of Pd $2p_{3/2}$ region. Reduced surface with both oxide and metallic contribution in black and PdO film over Pd in red.

Electrochemistry

The electrochemical experiments were controlled with a Bio-Logic SP200 potentiostat and were performed in a custom-made single compartment cell in three-electrode configuration (see Figure S6): a leak-free Ag/AgCl (Harvard Instruments) reference electrode was used, a platinum mesh served as counter electrode, and a Pd thin film (~5 nm) sputtered onto graphene sheets was used as working electrode (see above for preparation details of the working electrode). The electrolyte was a phosphate buffer, pH 2.83, which was prepared by partially neutralizing a 0.1 M H_3PO_4 solution with 2.5 M NaOH. Prior to any electrochemical or spectro-electrochemical measurement, the electrolyte was saturated with either nitrogen or propene gas for ca. 15 min while the potential was held at 0.68 V vs. RHE (the gas was kept flowing during the measurements).

The Pd/graphene working electrodes were characterized electrochemically by cyclic voltammetry in phosphate buffer with the electrolyte either saturated with nitrogen or propene gas (Fig. S4). The voltammogram acquired in N_2-saturated electrolyte shows the characteristic features of palladium, a broad oxidative wave starting at ca. 0.8 V vs. RHE arising from electrochemically induced adsorption of OH(ad)/O(ad),[3,4] and a sharp reductive peak at ca. 0.7 V vs. RHE. Upon saturating the electrolyte with propene gas, the voltammetric feature attributed to electrodeposition of OH(ad)/O(ad) is initially suppressed, suggesting that the propene has adsorbed on the palladium surface.[5] At potentials above ca. 1.0 V, the anodic current is higher than in N_2 saturated electrolyte. The additional current is assumed to derive from the oxidation of propene.[5] The cathodic peak ascribed to PdO reduction is suppressed in propene in comparison with N_2, indicating that the oxidation of Pd is decreased in the presence of propene. This corroborates to the interpretation that the additional oxidative current in propene is due to propene oxidation.

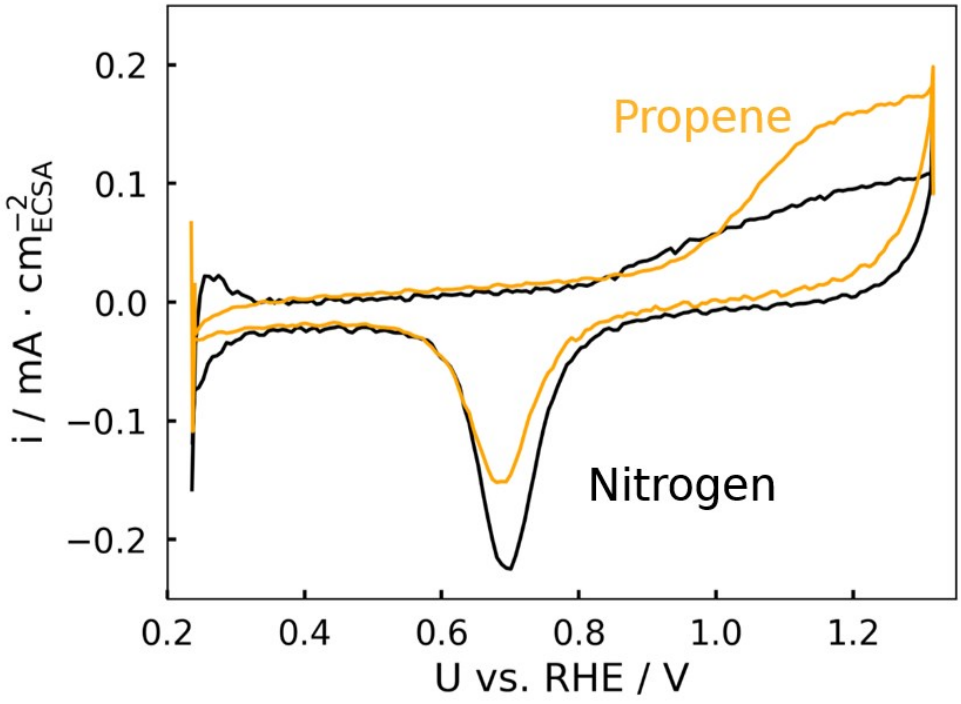

Figure S4. Cyclic voltammetry of palladium thin film sputtered on conductive graphene, acquired at 50 mV s^{-1} in either nitrogen-saturated or propene-saturated phosphate buffer pH 2.83 (total phosphate concentration: 0.1 M). The ESCA was calculated from the PdO reduction peak (for the CV in N_2), or the double layer capacitance (for the CV in propene, as the PdO reduction peak is affected by the presence of propene).

Previous knowledge on reaction mechanism

The mechanistic discussion in this paper relies to a significant extent on data and interpretations published previously by Winiwarter et al.[5] The most important conclusions of that work are the following:

- The product distribution of propene oxidation on Pd depends on the applied potential: Between 0.7-1.0 V vs RHE, allyl oxidation to allyl alcohol, acrolein, and acrylic dominates, while at higher potentials between 1.0V and 1.2V vs RHE, propylene glycol, a vinyl oxidation product is the major liquid product.
- Reaction onset at ca. 0.7 V vs RHE coincides with activation of water on Pd, as demonstrated both experimentally and using DFT calculations. This indicates that OH/O activation on the surface is critical for the reaction.
- However, under reaction conditions, the surface is populated by propene adsorbates: Due to Pd's carbophilicity, there is a thermodynamic driving force for consecutive oxidative deprotonation of propene in allyl position if adsorbed through the allyl carbon, and deprotonation and breaking of C-C bonds if adsorbed through the double bond, leading to irreversibly retained, unreactive adsorbates. The presence of these adsorbates under reaction conditions was confirmed experimentally.
- Therefore, the authors concluded that the reaction proceeds via the Langmuir-Hinshelwood mechanism.
- Finally, the selectivity towards allyl oxidation products is steered by the adsorption mechanism, which is influenced by non-reactive propene-derived adsorbates at the surface.

Product analysis

While Winiwarter et al. [5] perform experiments in 0.1M $HClO_4$, in this work we used phosphate buffer to avoid X-ray absorption by the electrolyte in the desired energy range. Figure S5 compares the faradaic efficiency for propene oxidation products in 0.1M $HClO_4$ and phosphate buffer at pH 2.3 on high surface area Pd electrodes prepared by electrodepositon. There are no significant differences in product distribution in the different electrolytes at lower potentials where allyl oxidation dominates. CVs shown in Figure S4 and by Winiwarter et al. indicate an oxidized surface and generally similar behavior when going to potentials above 1.1 V vs RHE. We therefore argue that the product distribution will also be significantly changed at potentials above 1.1 V vs RHE in phosphate buffer, as demonstrated for 0.1M $HClO_4$.

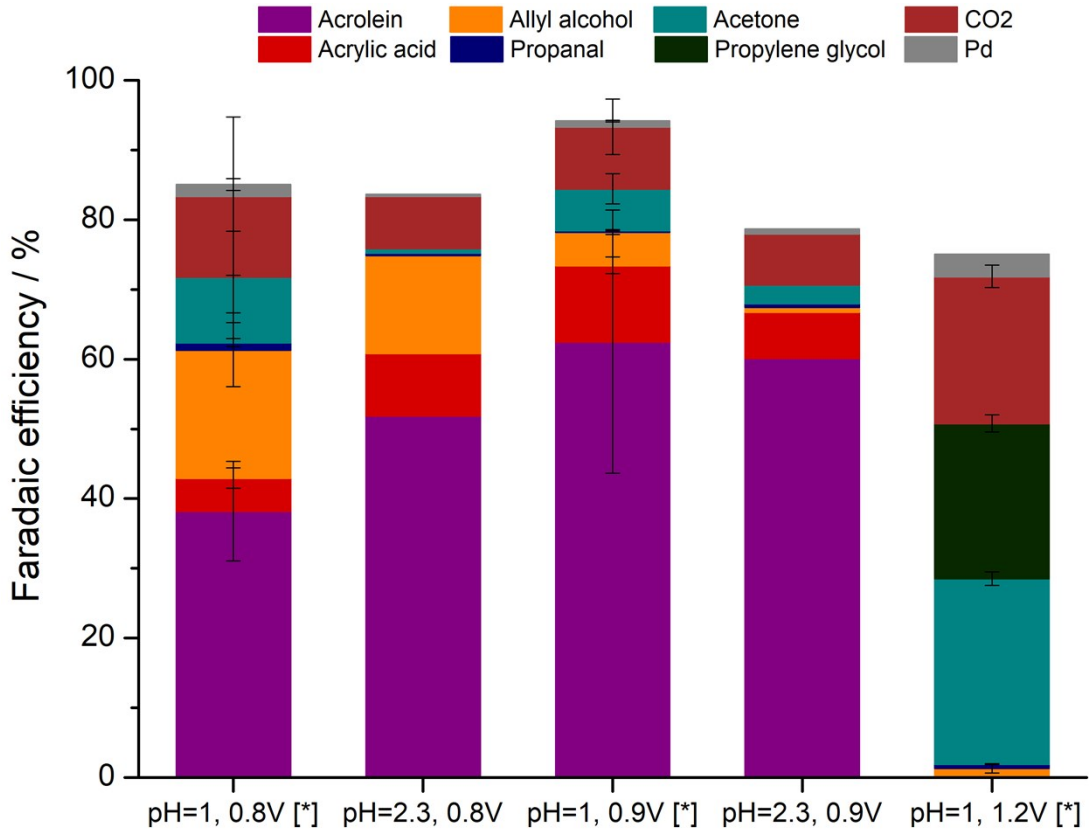

Figure S5 Faradaic efficiency for propene oxidation products at pH 1 (0.1M HCl, [*] data as published in ref. [5]) compared with pH 2.3 (phosphate buffer) on high surface area Pd electrodes. All experiments were performed in a glass H-cell. First the cell was purged with propene while holding the potential constant at 0.4 V vs. RHE, after which the potential was stepped to the potential shown in the axis labels and held for 1h. Products were quantified using HPLC, HS-GC and NMR. The same experimental procedure was followed for the measurements at pH 2.3 as described in ref. [5] The formation of acetone is not considered in the mechanistic discussion in the present paper, as it is formed by homogeneous reaction with dissolved Pd^{2+} via a Wacker-type mechanism.

X-ray absorption spectroscopy

The in-situ Pd L-edge XAS spectra were obtained at beamline 4-3 at SSRL. Figure S6 shows the schematic images of the experimental setup. Measurements were done in He environment by scanning X-ray energy and detecting Pd fluorescence using a silicon drift detector. The XAS spectra were normalized by the incident X-ray flux ($\sim 10^{12}$ ph/s) measured before the sample for each energy

step. The Si(111) double-crystal monochromator resolution was ~0.25 eV and the energy scale was calibrated to the (Pd) white line peak at 3173 eV. The electrochemical cell was installed at the angle of ~10° (to the surface normal) that both the incident beam and the florescence beam penetrating through the working electrode to avoid interaction with the electrolyte. Radiation damage was assessed by monitoring spectral changes upon successive scans at one sample position, and no damage was observed during application of an external potential. A second order polynomial baseline (fit at energies < 3130 eV) was subtracted and the spectra were normalized to 1 in the average absorbance from 3225 to 3325 eV, where the per Pd cross section is assumed to be invariant. The average spectra of at least 3 sample positions or more are reported in Figure 1 A,B.

The energy resolution of Pd L_3-edge XAS is constrained by the lifetime of the 2p core hole (Γ~2 eV). Previous *in-situ* study on Pt nanoparticles[6] shows that spectral signatures of different chemisorbed species can be identified by high energy resolution florescence detection which gives comparable spectral resolution to conventional Pd L_3-edge XAS. Additionally, in order to minimize the background contribution of bulk Pd atoms, the thin catalyst was prepared by sputtering Pd onto a foreign conductive graphene sheet (see above) instead of using thick electrode.

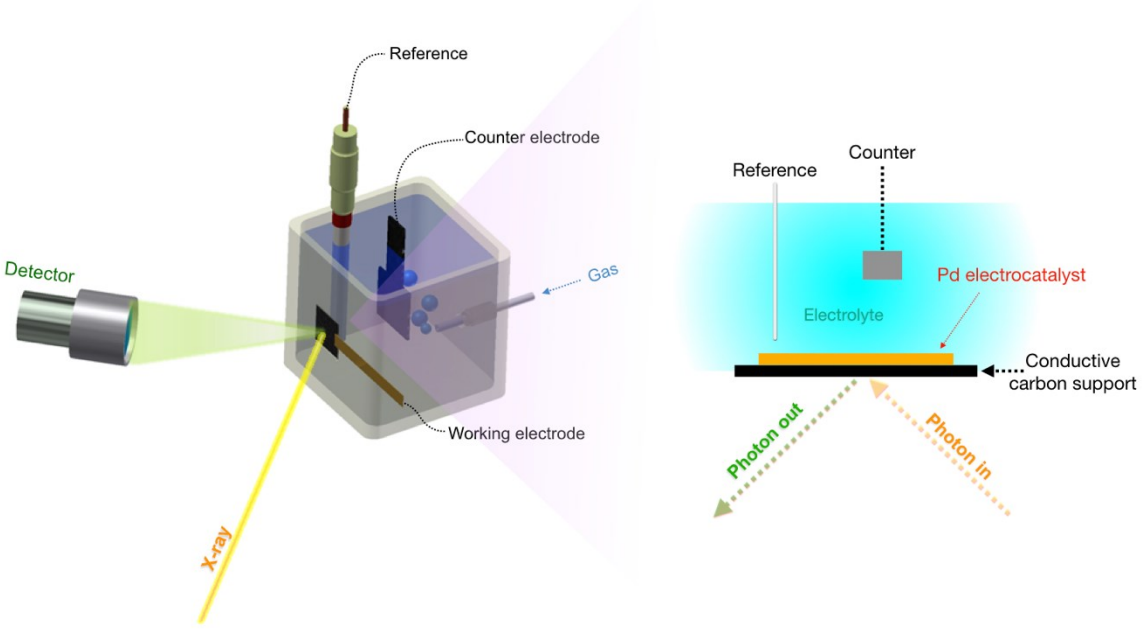

Figure S6: Schematic view of the electrochemical cell for operando XAS experiment

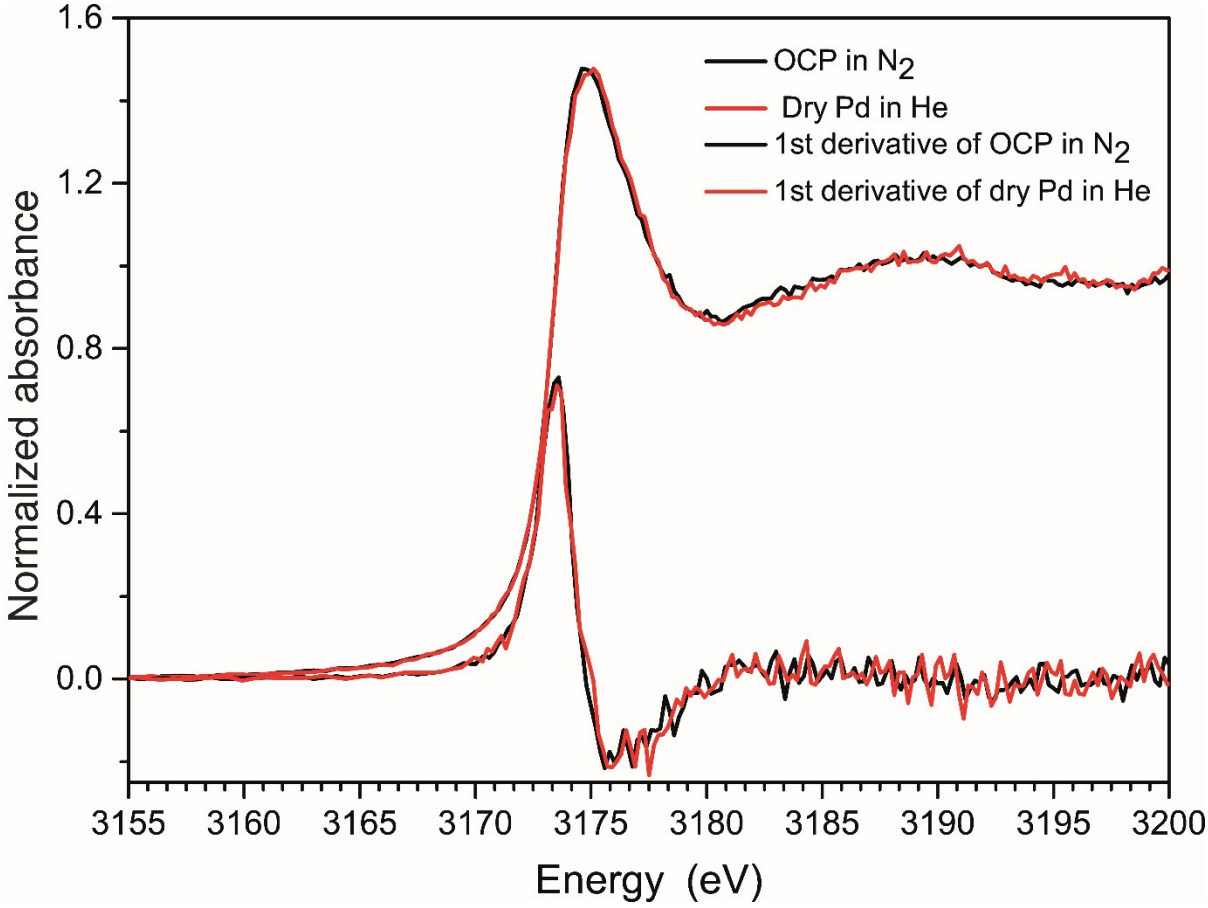

Figure S7: In situ Pd L_3-edge XAS spectra and first derivative of them in the rising-edge energy region for dry Pd in He environment(black) and open circuit potential in N_2 saturated electrolyte (red)

Modelling the electrochemical interface of Pd(111)

Computational details

To compare the thermodynamic stability of different surface adsorbed states at the Pd-electrolyte interface as a function of the electrode potential, we employ DFT augmented with the generalized computational hydrogen electrode (GCHE) method. This allows us to control the pH (set to 2.83) and gas phase partial pressures while varying the potential and provides us with information on the prevalent composition at the Pd interface for a given experimental condition. More specifically, we study the effects of varying the reaction mixture in the gas phase (1 bar N_2 atmosphere versus 1 bar propene atmosphere), as well as the potential effect in the region around where propene oxidation is seen experimentally (i.e, 0.5 to 1.5 U_{RHE}). Pd fcc(111) is the least reactive Pd facet. As the reaction is limited by the presence of carbon, we expect that any more reactive facet than fcc(111) would be even more prone to carbon poisoning.[5] Therefore, we argue that the reaction will primarily take place on the fcc(111) facet. Also, we expect Pd fcc(111) to be the most abundant facet on polycrystalline Pd, since it has the lowest surface energy of all Pd facets. [7]

The computational details follow the same theoretical framework as outlined in our recent papers.[8,9] In summary, we compute the energetics of a number of adsorbates and coverages adsorbed onto the

Pd(111) facet. The considered adsorbates are H_2O, OH, O, N, N_2, C, CO, and C_3H_6 (Pr=propene) in aqueous environment with a varying degree of coverage and deprotonation. We also investigate mixed phases of Pr, OH, and CO, as well as the formation of a thin PdO oxide layer. We use DFT at the PBE+D3(BJ) level of theory[10–12] and the VASP program suit throughout.[13] Low-energy structures are determined on a periodic three-layers-thick slab model with three additional layers of explicit water solvent molecules added ontop starting from structures identified on the Cu(111) surface in a previous study.[9] The top layer of Pd is allowed to relax in the optimizations. All calculations are carried out on a 2×3 surface supercell model.

The water and adsorbate structures above are subsequently sampled dynamically with *ab initio* molecular dynamics (AIMD). Here all Pd atoms are kept fixed. Each structure gives rise to a different work function (W_F) and free energy (G=E_{DFT}+*ZPE*). The G consists of the DFT energy, E_{DFT}, and the zero-point energy (*ZPE*). The ZPE is obtained from vibrational analysis (as described in reference[14]) of the low-energy adsorbates without water solvation. The W_F is computed by

$$W_F = V_v - E_F/e. \quad (1)$$

Above, E_F and e are the Fermi energy and elementary charge, respectively. V_V is the electrostatic potential in vacuum in close proximity to the surface. Here V_V is set to the potential of the vacuum space in between the periodic slabs using dipole corrections[15]. We can then relate the W_F and G to the potential (U) and *pH* of the system using the computational hydrogen electrode[16] and the experimental value[17] of the work function of the standard hydrogen electrode ($W_{F,SHE}$ = 4.44 eV) as references. With this procedure, we can express the free energy for the interfacial system, G^{int}, via the GCHE[18] by

$$G^{int} = G(\Delta n) - G^{int}_{ref}(\Delta n = 0) - \Delta n \cdot \left(\frac{\mu^{\circ}_{H_2}}{2} - eU_{RHE}\right) \quad (2)$$

We define $\Delta n = n - n_0$, where n is the number of protons in the studied state and n_0 the number of protons in a reference state consisting of a pure water-palladium interface G^{int}_{ref}. In other words, Δn reflects the addition or removal of protons to the system with respect to the neutral reference state. In the above, n_0 is taken as the number of H in the water layer bonded to the surface, which is 12 for the studied system corresponding to six adsorbed H_2O. This will also be used to define a monolayer (ML): each surface supercell can adsorb up to six species. The exception is the bulky propene molecule of which only four molecules can be co-adsorbed in one supercell. We also note that one ML (six adsorbates) is only half of the available surface Pd atomic sites (i.e. 12).

We include the standard chemical potential of H_2, $\mu^{o}_{H_2}$, in a manner similar to the other adsorbates (see below) by obtaining free-energy corrections from the NIST-JANAF tables.[19] The potential of the reversible hydrogen electrode (U_{RHE}), and standard hydrogen electrode (U_{SHE}), are related through

$$eU_{RHE} = eU_{SHE} + 2.3\ k_B T\ pH = W_F - W_{F,SHE} + 2.3\ k_B T\ pH \quad (3)$$

where T is the temperature (298.15 K) and k_B the Boltzmann constant. For the N_2 and propene derived adsorbates, we relate the energies to the respective gas-phase molecules. The total interface energy for the adsorbate system, G^{int}_{ads}, is evaluated by

$$G_{ads}^{int} = G^{int} - \overbrace{\Delta n_{propene}\,\mu_{propene}}^{Propene} - \overbrace{\Delta n_{N_2}\,\mu_{N_2}}^{N_2} \quad (4)$$

G^{int} is determined by eqn. 2 and Δn_x , x=propene or N_2, can be a fractional number, e.g. when propene leads to C* or CO*. The chemical potential μ_i^o of the adsorbate reference molecules N_2 and propene is computed by

$$\mu_i(T) = E_{DFT,i} + ZPE_i + \Delta\mu_i^0(T^0,p^0) \quad (5)$$

for which corrections to the standard state of 1 bar and 298.15 K are taken from the NIST-JANAF tables[19] and from D'Ans and Lax.[20] The final energies are normalized by the number of exposed palladium atoms at the surface, i.e. 12.

The adsorbed states were considered by the below reactions:

$C_3H_6(g) + * \rightarrow C_3H_5* + (H^+ + e^-)$ (Propene adsorption)

$C_3H_6(g) + 3* \rightarrow 3C* + 6(H^+ + e^-)$ (Carbon formation)

$C_3H_6(g) + 3H_2O + 3* \rightarrow 3CO* + 12(H^+ + e^-)$ (Carbon monoxide generation)

$3⅓C_3H_6(g) + 2\,H_2O + 5* \rightarrow 3C_3H_5* + CO* + OH* + 8(H^+ + e^-)$ (Mixed adsorption)

$H_2O(l) + * \rightarrow OH* + (H^+ + e^-)$ (Surface hydroxylation)

$H_2O(l) + * \rightarrow O* + 2(H^+ + e^-)$ (Surface oxidation)

$Pd + H_2O(l) \rightarrow PdO + 2(H^+ + e^-)$ (Surface oxide formation)

$N_2(g) + * \rightarrow N_2*$ (Molecular nitrogen adsorption)

$½N_2(g) + * \rightarrow N*$ (Dissociative nitrogen adsorption)

In all calculations a plane-wave basis set with a 400 eV cut-off was used to evaluate the valence states. The ionic cores were represented by standard PAW potentials.[21,22] To evaluate the final energies and work-functions, we used a Γ-centered 4×4×1 **k**-point mesh and the Methfessel-Paxton[23] approach with a Gaussian width of 0.2 eV. The AIMD simulations were run at the same level of theory for 1 ps with a time step of 1 fs, but using only the Γ-point and no dipole corrections. We have previously found that 1 ps is sufficient for the sampling given well-optimized low-energy interface start structures.[8]

Results

Figure S8 shows the stability of all the considered states as a function of applied potential. Figure 2 of the main article includes the same results, while displaying only the prevailing states for each type of adsorbate and divided into N_2 and propene atmosphere.

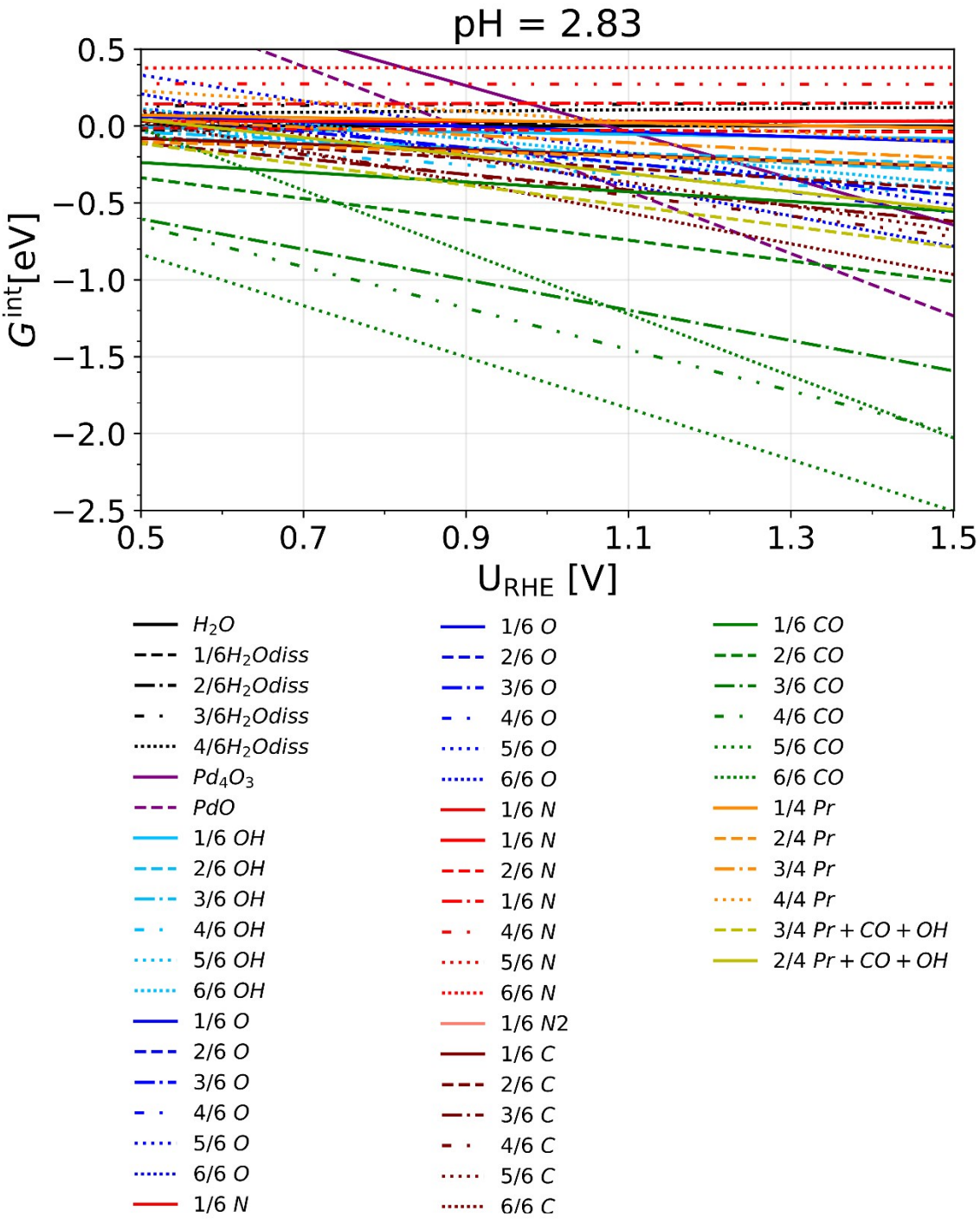

Figure S8. Computed stability of surface species on Pd(111) at 298K and pH 2.83 for the various adsorbates and coverages considered in this study.

One can see that in a 1 bar N_2 atmosphere, the most favorable adsorption state is 2/3ML of OH* up to approximately 1.0 V_{RHE}. Thereafter a full ML of O* is stable for a small potential window (0.99-1.06 V_{RHE}, from our calculations), after which the surface is oxidized into PdO. Note that the accuracy of the calculated transitions is around 0.1-0.2 V. [8,9,24]

For a 1 bar propene atmosphere, the situation becomes more involved as propene can be oxidized into many different species/intermediates. Thermodynamically, CO* is the most stable surface species for all potentials. However, its oxidation into CO_2 has not been accounted for in the presented data,

and CO is expected to be stripped off at potentials around and above 0.9 V_{RHE}.[5] It is also possible that CO formation is kinetically hindered at lower potentials, which is why it becomes necessary to consider the possibility of less oxidized carbonaceous surface species. After CO*, C* and Pr* (deprotonated propene) are the most stable at low potentials. ½ ML of Pr* is the most stable surface species up to approximately ~0.5 V_{RHE} and, when comparing to the case of N_2 atmosphere, will replace OH*. Around this potential (~0.5 V_{RHE}), ½ ML of C* becomes more stable than pure Pr* surface states (based only on thermodynamic arguments, kinetics omitted). However, C* is of similar stability as a mixed ¾ Pr* + 1/6 OH* + 1/6 CO* state. The latter is a state that has been recently suggested to be present under operational conditions for propene oxidation over Pd.[5] This state competes with ½-1ML C* up until 1.1-1.2 V_{RHE}, when PdO becomes the most stable species. In other words, the propene-derived adsorbates may prevent surface oxidation up to around 1.2 V_{RHE}.

Lastly, it is important to point out that the surface coverage of the propene-derived species can only be accessed through a microkinetic model based on accurate data of all the relevant surface reactions. Such an analysis is, however, beyond the scope of the present study.

Multiple-Scattering Calculations

All X-ray absorption spectroscopy calculations were modeled using the FEFF code, which employs an *ab initio* multiple-scattering formalism.[25] By using the ”COREHOLE none” card, potential and phase shift were calculated assuming complete screening of the core-hole, resulting in better agreement with experimental Pd L_3-edge intensity that is consistent with previous reported FEFF L_3-edge XAS results for transition metals.[6,26,27] The “SCF” radius for all calculations was set to R_{SCF}= 4 Å to include at least one surface unit cell. A “FMS” radius of 6 Å was found to be optimal to prevent that scattering paths are neglected and to ensure convergence of the multiple-scattering calculations for the Pd and PdO structures. Since all of the Pd atoms of each structure contribute to the spectrum, the average of their individual spectra is presented in Figure 1C of the main text as well as in Figures S9 and S10.

All chemisorbed adlayers were constructed on the Pd (111) surface of a 125-atom slab comprising (5 x 5) surface units and 5 atomic layers. The structures of Pd and PdO were obtained from Materials project (https://materialsproject.org/).[28] The “ION” card was used only for surface oxide to add extra ionicity value of 0.01 to the top-most atomic layer. The resulting spectrum (1 x 5 x 5; with “ION” card) was averaged with bulk spectra (4 x 5 x 5) resulting in spectra shown in Fig 1C (surface oxide).

Surface configurations for all hypothetical adsorbates were constructed on the top most atomic layer of Pd adsorbent. The adsorbates consist of different species such as O, OH, CO or C_3H_6 on unreconstructed Pd(111). The geometry of these hypothetical structures was not optimized and adsorbate and strain-induced relaxation was neglected. Adsorption sites, Pd – adsorbate bond distances were contracted to match the known reference structures[28] and structures are shown below.

Comparing calculated XAS spectra for DFT optimized (see below) and non-optimized structures showed no significant difference in the Pd white line intensity, see Figure S9. Therefore, structure optimization of adsorbate structures was not performed for the presented spectra in the main text (Fig. 1C). The environment at the surface in the electrolyte is also expected to differ from structure optimization at perfect vacuum at 0 K.

The Pd surface-oxide structure is taken from Gustafsson et al.[29] and was optimized using the Perdew-Burke-Ernzerhof[12] DFT-functional as implemented in the Vienna Ab initio Simulation Package (VASP).[13] The single PdO overlayer with a (√5×√5)R27° reconstruction pattern was placed on a periodic three

layers thick Pd-slab with a 13.75 × 13.75 $Å^2$ surface supercell. A 25 Å vacuum distance was employed, and the bottom layer was frozen during the relaxation. The valence states (Pd: $5s^1 4d^9$, O: $2s^2 2p^4$) were expanded in a plane-wave basis-set with an energy cut-off of 500 eV, whereas the core electrons were represented by standard PAW potentials.[22] The convergence criteria were set to 10^{-6} eV and 10^{-2} eV/Å for the SCF cycles and ionic forces, respectively. The Brillouin zone was sampled on a Γ-centered 4×4×1 **k**-mesh using the first-order Methfessel-Paxton smearing scheme.[23]

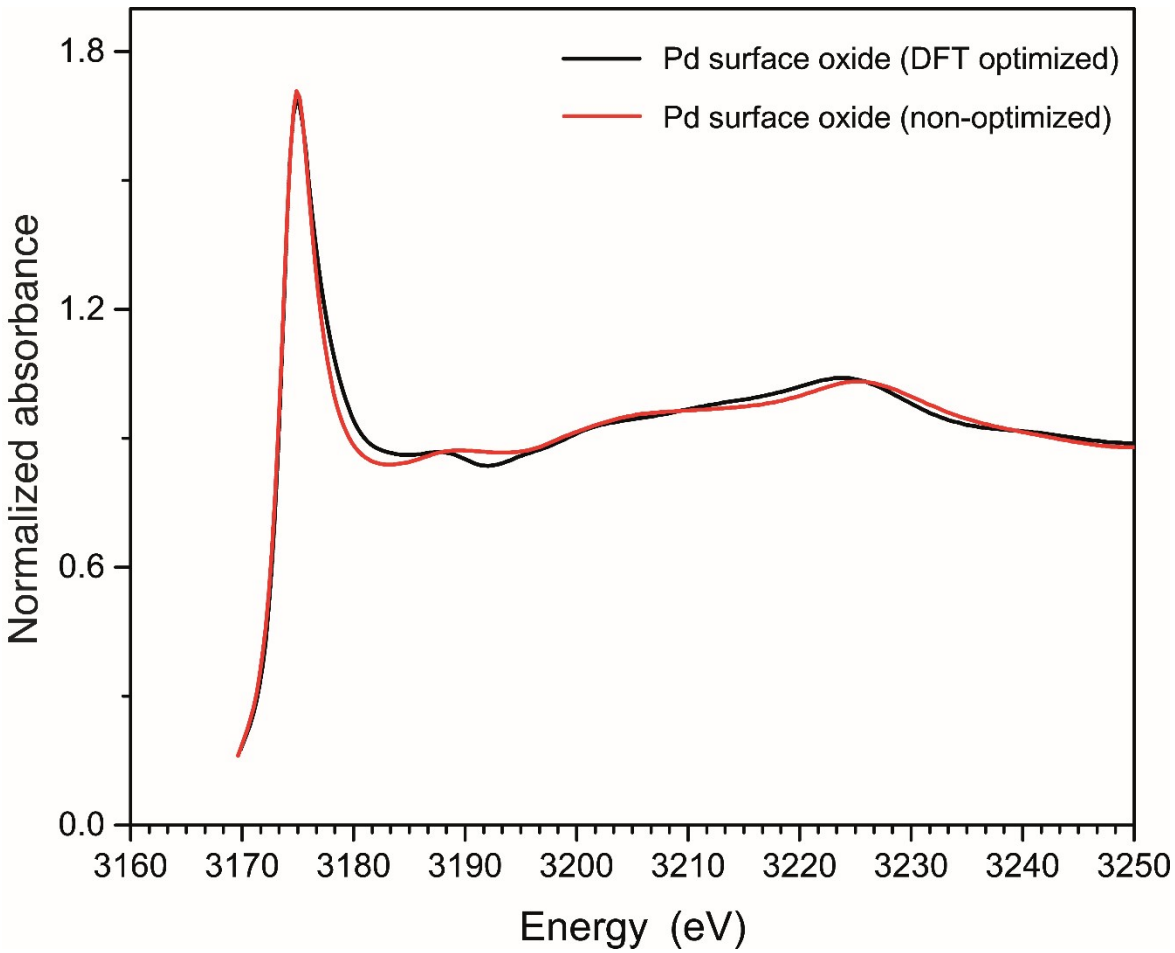

Figure S9. Comparison of the simulated Pd L_3-edge XAS using FEFF for DFT optimized Pd surface oxide structure (black) vs non-optimized Pd surface oxide (red)

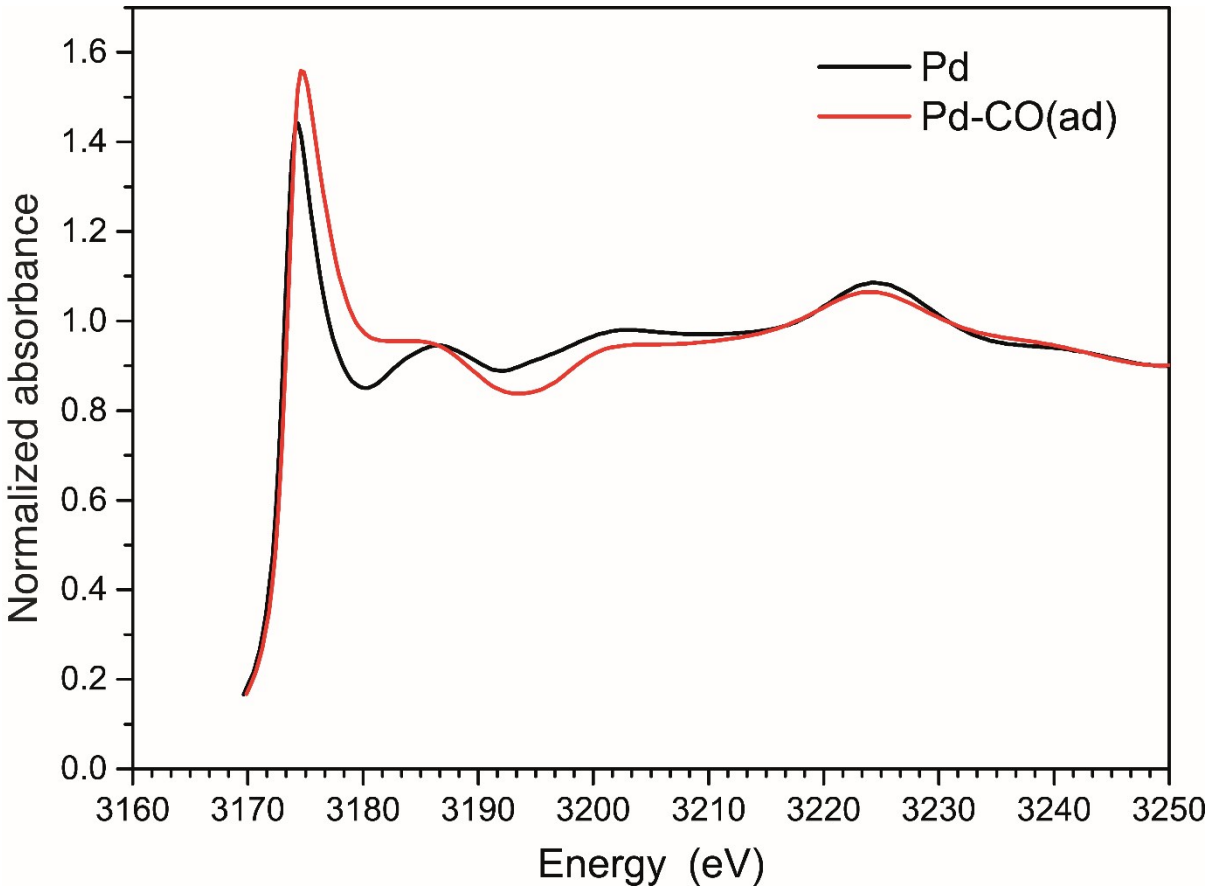

Figure S10. Simulated spectra of the Pd L_3-edge XAS using FEFF for clean Pd surface (black) and Pd surface covered by CO (red)

Adsorption properties of propylene oxide on PdO

We propose that the oxidation of propane over palladium oxide leads to the generation of propene glycol via a propylene oxide (epoxide) intermediate, see Figure 3 of the main text. While the full mechanism for the formation of propylene oxide is beyond the scope of this paper, we investigate whether or not the oxidation of propylene oxide to propylene glycol is a solution or surface mediated transformation by studying the adsorption behavior of propylene oxide onto our PdO DFT model. A number of initial configurations were tested. In all cases, propene oxide spontaneously desorbs from the surface, dissolving in the aqueous solvent. Figure S11 shows a representative relaxation profile for propene oxide starting from a surface state.

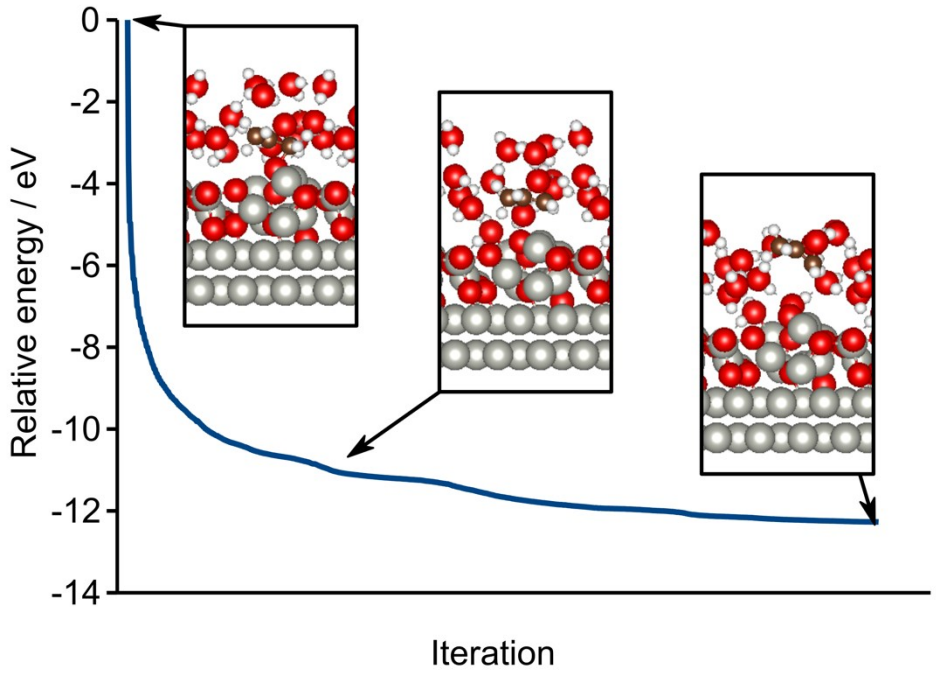

Figure S11. Example of a structural relaxation profile for propene oxide on the PdO covered Pd(111) surface.

The structures used for FEFF calculations

Pd

Atom	X	Y	Z
Pd	12.3778800000	11.9106190240	15.9834849480
Pd	9.6272400000	11.9106190240	15.9834849480
Pd	6.8766000000	11.9106190240	15.9834849480
Pd	4.1259600000	11.9106190240	15.9834849480
Pd	1.3753200000	11.9106190240	15.9834849480
Pd	11.0025600000	9.5285809760	15.9834849480
Pd	8.2519200000	9.5285809760	15.9834849480
Pd	5.5012800000	9.5285809760	15.9834849480
Pd	2.7506400000	9.5285809760	15.9834849480
Pd	0.0000000000	9.5285809760	15.9834849480
Pd	12.3778800000	7.14000000	15.9834849480
Pd	9.6272400000	7.14000000	15.9834849480
Pd	6.8766000000	7.14000000	15.9834849480
Pd	4.1259600000	7.14000000	15.9834849480
Pd	1.3753200000	7.14000000	15.9834849480
Pd	11.0025600000	4.7642190240	15.9834849480
Pd	8.2519200000	4.7642190240	15.9834849480
Pd	5.5012800000	4.7642190240	15.9834849480
Pd	2.7506400000	4.7642190240	15.9834849480
Pd	0.0000000000	4.7642190240	15.9834849480
Pd	12.3778800000	2.3821809760	15.9834849480
Pd	9.6272400000	2.3821809760	15.9834849480
Pd	6.8766000000	2.3821809760	15.9834849480
Pd	4.1259600000	2.3821809760	15.9834849480
Pd	1.3753200000	2.3821809760	15.9834849480
Pd	11.0025600000	11.1166539840	13.7377573920
Pd	8.2519200000	11.1166539840	13.7377573920
Pd	5.5012800000	11.1166539840	13.7377573920
Pd	2.7506400000	11.1166539840	13.7377573920
Pd	0.0000000000	11.1166539840	13.7377573920
Pd	12.3778800000	8.7344730080	13.7377573920
Pd	9.6272400000	8.7344730080	13.7377573920
Pd	6.8766000000	8.7344730080	13.7377573920
Pd	4.1259600000	8.7344730080	13.7377573920
Pd	1.3753200000	8.7344730080	13.7377573920
Pd	11.0025600000	6.3522920320	13.7377573920
Pd	8.2519200000	6.3522920320	13.7377573920
Pd	5.5012800000	6.3522920320	13.7377573920
Pd	2.7506400000	6.3522920320	13.7377573920
Pd	0.0000000000	6.3522920320	13.7377573920
Pd	12.3778800000	3.9702539840	13.7377573920
Pd	9.6272400000	3.9702539840	13.7377573920
Pd	6.8766000000	3.9702539840	13.7377573920
Pd	4.1259600000	3.9702539840	13.7377573920
Pd	1.3753200000	3.9702539840	13.7377573920
Pd	11.0025600000	1.5880730080	13.7377573920

Pd	8.2519200000	1.5880730080	13.7377573920
Pd	5.5012800000	1.5880730080	13.7377573920
Pd	2.7506400000	1.5880730080	13.7377573920
Pd	0.0000000000	1.5880730080	13.7377573920
Pd	12.3778800000	10.32250160	11.4918000000
Pd	9.6272400000	10.32250160	11.4918000000
Pd	6.8766000000	10.32250160	11.4918000000
Pd	4.1259600000	10.32250160	11.4918000000
Pd	1.3753200000	10.32250160	11.4918000000
Pd	11.0025600000	7.9405079680	11.4918000000
Pd	8.2519200000	7.9405079680	11.4918000000
Pd	5.5012800000	7.9405079680	11.4918000000
Pd	2.7506400000	7.9405079680	11.4918000000
Pd	0.0000000000	7.9405079680	11.4918000000
Pd	12.3778800000	5.5583269920	11.4918000000
Pd	9.6272400000	5.5583269920	11.4918000000
Pd	6.8766000000	5.5583269920	11.4918000000
Pd	4.1259600000	5.5583269920	11.4918000000
Pd	1.3753200000	5.5583269920	11.4918000000
Pd	11.0025600000	3.17610160	11.4918000000
Pd	8.2519200000	3.17610160	11.4918000000
Pd	5.5012800000	3.17610160	11.4918000000
Pd	2.7506400000	3.17610160	11.4918000000
Pd	0.0000000000	3.17610160	11.4918000000
Pd	12.3778800000	0.7941079680	11.4918000000
Pd	9.6272400000	0.7941079680	11.4918000000
Pd	6.8766000000	0.7941079680	11.4918000000
Pd	4.1259600000	0.7941079680	11.4918000000
Pd	1.3753200000	0.7941079680	11.4918000000
Pd	12.3778800000	11.9106190240	9.2458426080
Pd	9.6272400000	11.9106190240	9.2458426080
Pd	6.8766000000	11.9106190240	9.2458426080
Pd	4.1259600000	11.9106190240	9.2458426080
Pd	1.3753200000	11.9106190240	9.2458426080
Pd	11.0025600000	9.5285809760	9.2458426080
Pd	8.2519200000	9.5285809760	9.2458426080
Pd	5.5012800000	9.5285809760	9.2458426080
Pd	2.7506400000	9.5285809760	9.2458426080
Pd	0.0000000000	9.5285809760	9.2458426080
Pd	12.3778800000	7.14000000	9.2458426080
Pd	9.6272400000	7.14000000	9.2458426080
Pd	6.8766000000	7.14000000	9.2458426080
Pd	4.1259600000	7.14000000	9.2458426080
Pd	1.3753200000	7.14000000	9.2458426080
Pd	11.0025600000	4.7642190240	9.2458426080
Pd	8.2519200000	4.7642190240	9.2458426080
Pd	5.5012800000	4.7642190240	9.2458426080
Pd	2.7506400000	4.7642190240	9.2458426080
Pd	0.0000000000	4.7642190240	9.2458426080
Pd	12.3778800000	2.3821809760	9.2458426080
Pd	9.6272400000	2.3821809760	9.2458426080

Pd	6.8766000000	2.3821809760	9.2458426080
Pd	4.1259600000	2.3821809760	9.2458426080
Pd	1.3753200000	2.3821809760	9.2458426080
Pd	11.0025600000	11.1166539840	7.0001150520
Pd	8.2519200000	11.1166539840	7.0001150520
Pd	5.5012800000	11.1166539840	7.0001150520
Pd	2.7506400000	11.1166539840	7.0001150520
Pd	0.0000000000	11.1166539840	7.0001150520
Pd	12.3778800000	8.7344730080	7.0001150520
Pd	9.6272400000	8.7344730080	7.0001150520
Pd	6.8766000000	8.7344730080	7.0001150520
Pd	4.1259600000	8.7344730080	7.0001150520
Pd	1.3753200000	8.7344730080	7.0001150520
Pd	11.0025600000	6.3522920320	7.0001150520
Pd	8.2519200000	6.3522920320	7.0001150520
Pd	5.5012800000	6.3522920320	7.0001150520
Pd	2.7506400000	6.3522920320	7.0001150520
Pd	0.0000000000	6.3522920320	7.0001150520
Pd	12.3778800000	3.9702539840	7.0001150520
Pd	9.6272400000	3.9702539840	7.0001150520
Pd	6.8766000000	3.9702539840	7.0001150520
Pd	4.1259600000	3.9702539840	7.0001150520
Pd	1.3753200000	3.9702539840	7.0001150520
Pd	11.0025600000	1.5880730080	7.0001150520
Pd	8.2519200000	1.5880730080	7.0001150520
Pd	5.5012800000	1.5880730080	7.0001150520
Pd	2.7506400000	1.5880730080	7.0001150520
Pd	0.0000000000	1.5880730080	7.0001150520

Pd low OH coverage

Atom	X	Y	Z
Pd	0.00000	1.58807	7.00012
Pd	2.75064	1.58807	7.00012
Pd	5.50128	1.58807	7.00012
Pd	8.25192	1.58807	7.00012
Pd	11.00256	1.58807	7.00012
Pd	1.37532	3.97025	7.00012
Pd	4.12596	3.97025	7.00012
Pd	6.87660	3.97025	7.00012
Pd	9.62724	3.97025	7.00012
Pd	12.37788	3.97025	7.00012
Pd	0.00000	6.35229	7.00012
Pd	2.75064	6.35229	7.00012
Pd	5.50128	6.35229	7.00012
Pd	8.25192	6.35229	7.00012
Pd	11.00256	6.35229	7.00012
Pd	1.37532	8.73447	7.00012
Pd	4.12596	8.73447	7.00012
Pd	6.87660	8.73447	7.00012
Pd	9.62724	8.73447	7.00012
Pd	12.37788	8.73447	7.00012
Pd	0.00000	11.11665	7.00012
Pd	2.75064	11.11665	7.00012
Pd	5.50128	11.11665	7.00012
Pd	8.25192	11.11665	7.00012
Pd	11.00256	11.11665	7.00012
Pd	1.37532	2.38218	9.24584
Pd	4.12596	2.38218	9.24584
Pd	6.87660	2.38218	9.24584
Pd	9.62724	2.38218	9.24584
Pd	12.37788	2.38218	9.24584
Pd	0.00000	4.76422	9.24584
Pd	2.75064	4.76422	9.24584
Pd	5.50128	4.76422	9.24584
Pd	8.25192	4.76422	9.24584
Pd	11.00256	4.76422	9.24584
Pd	1.37532	7.140	9.24584
Pd	4.12596	7.140	9.24584
Pd	6.87660	7.140	9.24584
Pd	9.62724	7.140	9.24584
Pd	12.37788	7.140	9.24584
Pd	0.00000	9.52858	9.24584
Pd	2.75064	9.52858	9.24584
Pd	5.50128	9.52858	9.24584
Pd	8.25192	9.52858	9.24584
Pd	11.00256	9.52858	9.24584
Pd	1.37532	11.91062	9.24584
Pd	4.12596	11.91062	9.24584

Pd	6.87660	11.91062	9.24584
Pd	9.62724	11.91062	9.24584
Pd	12.37788	11.91062	9.24584
Pd	1.37532	0.79411	11.49180
Pd	4.12596	0.79411	11.49180
Pd	6.87660	0.79411	11.49180
Pd	9.62724	0.79411	11.49180
Pd	12.37788	0.79411	11.49180
Pd	0.00000	3.17615	11.49180
Pd	2.75064	3.17615	11.49180
Pd	5.50128	3.17615	11.49180
Pd	8.25192	3.17615	11.49180
Pd	11.00256	3.17615	11.49180
Pd	1.37532	5.55833	11.49180
Pd	4.12596	5.55833	11.49180
Pd	6.87660	5.55833	11.49180
Pd	9.62724	5.55833	11.49180
Pd	12.37788	5.55833	11.49180
Pd	0.00000	7.94051	11.49180
Pd	2.75064	7.94051	11.49180
Pd	5.50128	7.94051	11.49180
Pd	8.25192	7.94051	11.49180
Pd	11.00256	7.94051	11.49180
Pd	1.37532	10.32255	11.49180
Pd	4.12596	10.32255	11.49180
Pd	6.87660	10.32255	11.49180
Pd	9.62724	10.32255	11.49180
Pd	12.37788	10.32255	11.49180
Pd	0.00000	1.58807	13.73776
Pd	2.75064	1.58807	13.73776
Pd	5.50128	1.58807	13.73776
Pd	8.25192	1.58807	13.73776
Pd	11.00256	1.58807	13.73776
Pd	1.37532	3.97025	13.73776
Pd	4.12596	3.97025	13.73776
Pd	6.87660	3.97025	13.73776
Pd	9.62724	3.97025	13.73776
Pd	12.37788	3.97025	13.73776
Pd	0.00000	6.35229	13.73776
Pd	2.75064	6.35229	13.73776
Pd	5.50128	6.35229	13.73776
Pd	8.25192	6.35229	13.73776
Pd	11.00256	6.35229	13.73776
Pd	1.37532	8.73447	13.73776
Pd	4.12596	8.73447	13.73776
Pd	6.87660	8.73447	13.73776
Pd	9.62724	8.73447	13.73776
Pd	12.37788	8.73447	13.73776
Pd	0.00000	11.11665	13.73776
Pd	2.75064	11.11665	13.73776
Pd	5.50128	11.11665	13.73776

Pd	8.25192	11.11665	13.73776
Pd	11.00256	11.11665	13.73776
Pd	1.37532	2.38218	15.98348
Pd	4.12596	2.38218	15.98348
Pd	6.87660	2.38218	15.98348
Pd	9.62724	2.38218	15.98348
Pd	12.37788	2.38218	15.98348
Pd	0.00000	4.76422	15.98348
Pd	2.75064	4.76422	15.98348
Pd	5.50128	4.76422	15.98348
Pd	8.25192	4.76422	15.98348
Pd	11.00256	4.76422	15.98348
Pd	1.37532	7.140	15.98348
Pd	4.12596	7.140	15.98348
Pd	6.87660	7.140	15.98348
Pd	9.62724	7.140	15.98348
Pd	12.37788	7.140	15.98348
Pd	0.00000	9.52858	15.98348
Pd	2.75064	9.52858	15.98348
Pd	5.50128	9.52858	15.98348
Pd	8.25192	9.52858	15.98348
Pd	11.00256	9.52858	15.98348
Pd	1.37532	11.91062	15.98348
Pd	4.12596	11.91062	15.98348
Pd	6.87660	11.91062	15.98348
Pd	9.62724	11.91062	15.98348
Pd	12.37788	11.91062	15.98348
O	1.28474	11.91364	18.00284
O	6.89104	11.67149	17.98976
O	12.42917	11.67274	17.98928
O	12.29507	7.13165	18.00119
O	12.30401	2.69497	17.97637
O	6.97118	2.57562	17.99540
O	1.51632	2.34134	17.99680
O	1.67700	7.262	18.01797
O	6.92499	7.37502	18.00670
H	13.35161	11.63741	18.28720
H	7.80785	11.63400	18.30432
H	0.35664	11.91406	18.28486
H	6.01840	7.41375	18.34949
H	12.74970	1.96557	18.43488
H	0.81968	7.28830	18.47101
H	1.08267	1.54236	18.33515
H	6.53098	1.81937	18.41398
H	12.73858	6.33711	18.33719

Pd low O coverage

Atom	X	Y	Z
Pd	0.00000	1.58807	7.00012
Pd	2.75064	1.58807	7.00012
Pd	5.50128	1.58807	7.00012
Pd	8.25192	1.58807	7.00012
Pd	11.00256	1.58807	7.00012
Pd	1.37532	3.97025	7.00012
Pd	4.12596	3.97025	7.00012
Pd	6.87660	3.97025	7.00012
Pd	9.62724	3.97025	7.00012
Pd	12.37788	3.97025	7.00012
Pd	0.00000	6.35229	7.00012
Pd	2.75064	6.35229	7.00012
Pd	5.50128	6.35229	7.00012
Pd	8.25192	6.35229	7.00012
Pd	11.00256	6.35229	7.00012
Pd	1.37532	8.73447	7.00012
Pd	4.12596	8.73447	7.00012
Pd	6.87660	8.73447	7.00012
Pd	9.62724	8.73447	7.00012
Pd	12.37788	8.73447	7.00012
Pd	0.00000	11.11665	7.00012
Pd	2.75064	11.11665	7.00012
Pd	5.50128	11.11665	7.00012
Pd	8.25192	11.11665	7.00012
Pd	11.00256	11.11665	7.00012
Pd	1.37532	2.38218	9.24584
Pd	4.12596	2.38218	9.24584
Pd	6.87660	2.38218	9.24584
Pd	9.62724	2.38218	9.24584
Pd	12.37788	2.38218	9.24584
Pd	0.00000	4.76422	9.24584
Pd	2.75064	4.76422	9.24584
Pd	5.50128	4.76422	9.24584
Pd	8.25192	4.76422	9.24584
Pd	11.00256	4.76422	9.24584
Pd	1.37532	7.140	9.24584
Pd	4.12596	7.140	9.24584
Pd	6.87660	7.140	9.24584
Pd	9.62724	7.140	9.24584
Pd	12.37788	7.140	9.24584
Pd	0.00000	9.52858	9.24584
Pd	2.75064	9.52858	9.24584
Pd	5.50128	9.52858	9.24584
Pd	8.25192	9.52858	9.24584
Pd	11.00256	9.52858	9.24584
Pd	1.37532	11.91062	9.24584
Pd	4.12596	11.91062	9.24584
Pd	6.87660	11.91062	9.24584

Pd	9.62724	11.91062	9.24584
Pd	12.37788	11.91062	9.24584
Pd	1.37532	0.79411	11.49180
Pd	4.12596	0.79411	11.49180
Pd	6.87660	0.79411	11.49180
Pd	9.62724	0.79411	11.49180
Pd	12.37788	0.79411	11.49180
Pd	0.00000	3.17615	11.49180
Pd	2.75064	3.17615	11.49180
Pd	5.50128	3.17615	11.49180
Pd	8.25192	3.17615	11.49180
Pd	11.00256	3.17615	11.49180
Pd	1.37532	5.55833	11.49180
Pd	4.12596	5.55833	11.49180
Pd	6.87660	5.55833	11.49180
Pd	9.62724	5.55833	11.49180
Pd	12.37788	5.55833	11.49180
Pd	0.00000	7.94051	11.49180
Pd	2.75064	7.94051	11.49180
Pd	5.50128	7.94051	11.49180
Pd	8.25192	7.94051	11.49180
Pd	11.00256	7.94051	11.49180
Pd	1.37532	10.32255	11.49180
Pd	4.12596	10.32255	11.49180
Pd	6.87660	10.32255	11.49180
Pd	9.62724	10.32255	11.49180
Pd	12.37788	10.32255	11.49180
Pd	0.00000	1.58807	13.73776
Pd	2.75064	1.58807	13.73776
Pd	5.50128	1.58807	13.73776
Pd	8.25192	1.58807	13.73776
Pd	11.00256	1.58807	13.73776
Pd	1.37532	3.97025	13.73776
Pd	4.12596	3.97025	13.73776
Pd	6.87660	3.97025	13.73776
Pd	9.62724	3.97025	13.73776
Pd	12.37788	3.97025	13.73776
Pd	0.00000	6.35229	13.73776
Pd	2.75064	6.35229	13.73776
Pd	5.50128	6.35229	13.73776
Pd	8.25192	6.35229	13.73776
Pd	11.00256	6.35229	13.73776
Pd	1.37532	8.73447	13.73776
Pd	4.12596	8.73447	13.73776
Pd	6.87660	8.73447	13.73776
Pd	9.62724	8.73447	13.73776
Pd	12.37788	8.73447	13.73776
Pd	0.00000	11.11665	13.73776
Pd	2.75064	11.11665	13.73776
Pd	5.50128	11.11665	13.73776
Pd	8.25192	11.11665	13.73776

Pd	11.00256	11.11665	13.73776
Pd	1.37532	2.38218	15.98348
Pd	4.12596	2.38218	15.98348
Pd	6.87660	2.38218	15.98348
Pd	9.62724	2.38218	15.98348
Pd	12.37788	2.38218	15.98348
Pd	0.00000	4.76422	15.98348
Pd	2.75064	4.76422	15.98348
Pd	5.50128	4.76422	15.98348
Pd	8.25192	4.76422	15.98348
Pd	11.00256	4.76422	15.98348
Pd	1.37532	7.140	15.98348
Pd	4.12596	7.140	15.98348
Pd	6.87660	7.140	15.98348
Pd	9.62724	7.140	15.98348
Pd	12.37788	7.140	15.98348
Pd	0.00000	9.52858	15.98348
Pd	2.75064	9.52858	15.98348
Pd	5.50128	9.52858	15.98348
Pd	8.25192	9.52858	15.98348
Pd	11.00256	9.52858	15.98348
Pd	1.37532	11.91062	15.98348
Pd	4.12596	11.91062	15.98348
Pd	6.87660	11.91062	15.98348
Pd	9.62724	11.91062	15.98348
Pd	12.37788	11.91062	15.98348
O	1.28474	11.91364	18.00284
O	6.89104	11.67149	17.98976
O	12.42917	11.67274	17.98928
O	12.29507	7.13165	18.00119
O	12.30401	2.69497	17.97637
O	6.97118	2.57562	17.99540
O	1.51632	2.34134	17.99680
O	1.67700	7.262	18.01797
O	6.92499	7.37502	18.00670

Pd high O coverage

Atom	X	Y	Z
Pd	0.00000	1.58807	7.00012
Pd	2.75064	1.58807	7.00012
Pd	5.50128	1.58807	7.00012
Pd	8.25192	1.58807	7.00012
Pd	11.00256	1.58807	7.00012
Pd	1.37532	3.97025	7.00012
Pd	4.12596	3.97025	7.00012
Pd	6.87660	3.97025	7.00012
Pd	9.62724	3.97025	7.00012
Pd	12.37788	3.97025	7.00012
Pd	0.00000	6.35229	7.00012
Pd	2.75064	6.35229	7.00012
Pd	5.50128	6.35229	7.00012
Pd	8.25192	6.35229	7.00012
Pd	11.00256	6.35229	7.00012
Pd	1.37532	8.73447	7.00012
Pd	4.12596	8.73447	7.00012
Pd	6.87660	8.73447	7.00012
Pd	9.62724	8.73447	7.00012
Pd	12.37788	8.73447	7.00012
Pd	0.00000	11.11665	7.00012
Pd	2.75064	11.11665	7.00012
Pd	5.50128	11.11665	7.00012
Pd	8.25192	11.11665	7.00012
Pd	11.00256	11.11665	7.00012
Pd	1.37532	2.38218	9.24584
Pd	4.12596	2.38218	9.24584
Pd	6.87660	2.38218	9.24584
Pd	9.62724	2.38218	9.24584
Pd	12.37788	2.38218	9.24584
Pd	0.00000	4.76422	9.24584
Pd	2.75064	4.76422	9.24584
Pd	5.50128	4.76422	9.24584
Pd	8.25192	4.76422	9.24584
Pd	11.00256	4.76422	9.24584
Pd	1.37532	7.140	9.24584
Pd	4.12596	7.140	9.24584
Pd	6.87660	7.140	9.24584
Pd	9.62724	7.140	9.24584
Pd	12.37788	7.140	9.24584
Pd	0.00000	9.52858	9.24584
Pd	2.75064	9.52858	9.24584
Pd	5.50128	9.52858	9.24584
Pd	8.25192	9.52858	9.24584
Pd	11.00256	9.52858	9.24584
Pd	1.37532	11.91062	9.24584
Pd	4.12596	11.91062	9.24584
Pd	6.87660	11.91062	9.24584

Pd	9.62724	11.91062	9.24584
Pd	12.37788	11.91062	9.24584
Pd	1.37532	0.79411	11.49180
Pd	4.12596	0.79411	11.49180
Pd	6.87660	0.79411	11.49180
Pd	9.62724	0.79411	11.49180
Pd	12.37788	0.79411	11.49180
Pd	0.00000	3.17615	11.49180
Pd	2.75064	3.17615	11.49180
Pd	5.50128	3.17615	11.49180
Pd	8.25192	3.17615	11.49180
Pd	11.00256	3.17615	11.49180
Pd	1.37532	5.55833	11.49180
Pd	4.12596	5.55833	11.49180
Pd	6.87660	5.55833	11.49180
Pd	9.62724	5.55833	11.49180
Pd	12.37788	5.55833	11.49180
Pd	0.00000	7.94051	11.49180
Pd	2.75064	7.94051	11.49180
Pd	5.50128	7.94051	11.49180
Pd	8.25192	7.94051	11.49180
Pd	11.00256	7.94051	11.49180
Pd	1.37532	10.32255	11.49180
Pd	4.12596	10.32255	11.49180
Pd	6.87660	10.32255	11.49180
Pd	9.62724	10.32255	11.49180
Pd	12.37788	10.32255	11.49180
Pd	0.00000	1.58807	13.73776
Pd	2.75064	1.58807	13.73776
Pd	5.50128	1.58807	13.73776
Pd	8.25192	1.58807	13.73776
Pd	11.00256	1.58807	13.73776
Pd	1.37532	3.97025	13.73776
Pd	4.12596	3.97025	13.73776
Pd	6.87660	3.97025	13.73776
Pd	9.62724	3.97025	13.73776
Pd	12.37788	3.97025	13.73776
Pd	0.00000	6.35229	13.73776
Pd	2.75064	6.35229	13.73776
Pd	5.50128	6.35229	13.73776
Pd	8.25192	6.35229	13.73776
Pd	11.00256	6.35229	13.73776
Pd	1.37532	8.73447	13.73776
Pd	4.12596	8.73447	13.73776
Pd	6.87660	8.73447	13.73776
Pd	9.62724	8.73447	13.73776
Pd	12.37788	8.73447	13.73776
Pd	0.00000	11.11665	13.73776
Pd	2.75064	11.11665	13.73776
Pd	5.50128	11.11665	13.73776
Pd	8.25192	11.11665	13.73776

Pd	11.00256	11.11665	13.73776
Pd	1.37532	2.38218	15.98348
Pd	4.12596	2.38218	15.98348
Pd	6.87660	2.38218	15.98348
Pd	9.62724	2.38218	15.98348
Pd	12.37788	2.38218	15.98348
Pd	0.00000	4.76422	15.98348
Pd	2.75064	4.76422	15.98348
Pd	5.50128	4.76422	15.98348
Pd	8.25192	4.76422	15.98348
Pd	11.00256	4.76422	15.98348
Pd	1.37532	7.140	15.98348
Pd	4.12596	7.140	15.98348
Pd	6.87660	7.140	15.98348
Pd	9.62724	7.140	15.98348
Pd	12.37788	7.140	15.98348
Pd	0.00000	9.52858	15.98348
Pd	2.75064	9.52858	15.98348
Pd	5.50128	9.52858	15.98348
Pd	8.25192	9.52858	15.98348
Pd	11.00256	9.52858	15.98348
Pd	1.37532	11.91062	15.98348
Pd	4.12596	11.91062	15.98348
Pd	6.87660	11.91062	15.98348
Pd	9.62724	11.91062	15.98348
Pd	12.37788	11.91062	15.98348
O	1.28474	11.91364	18.00284
O	6.89104	11.67149	17.98976
O	12.42917	11.67274	17.98928
O	12.29507	7.13165	18.00119
O	12.30401	2.69497	17.97637
O	6.97118	2.57562	17.99540
O	1.51632	2.34134	17.99680
O	1.67700	7.262	18.01797
O	6.92499	7.37502	18.00670
O	3.47331	12.79131	17.68037
O	9.02973	12.84936	17.67014
O	9.66904	1.72178	17.89233
O	3.47253	3.10677	17.75562
O	9.28429	7.58399	17.92649
O	4.04345	7.02907	18.00115

Pd Surface oxide (non-optimized structures)
Top most atomic layer

Atom	X	Y	Z
Pd	1.37532	2.38218	15.98348
Pd	4.12596	2.38218	15.98348
Pd	6.87660	2.38218	15.98348
Pd	9.62724	2.38218	15.98348
Pd	12.37788	2.38218	15.98348
Pd	0.00000	4.76422	15.98348
Pd	2.75064	4.76422	15.98348
Pd	5.50128	4.76422	15.98348
Pd	8.25192	4.76422	15.98348
Pd	11.00256	4.76422	15.98348
Pd	1.37532	7.140	15.98348
Pd	4.12596	7.140	15.98348
Pd	6.87660	7.140	15.98348
Pd	9.62724	7.140	15.98348
Pd	12.37788	7.140	15.98348
Pd	0.00000	9.52858	15.98348
Pd	2.75064	9.52858	15.98348
Pd	5.50128	9.52858	15.98348
Pd	8.25192	9.52858	15.98348
Pd	11.00256	9.52858	15.98348
Pd	1.37532	11.91062	15.98348
Pd	4.12596	11.91062	15.98348
Pd	6.87660	11.91062	15.98348
Pd	9.62724	11.91062	15.98348
Pd	12.37788	11.91062	15.98348
O	11.49940	3.204	17.50217
O	9.06074	3.62969	17.52336
O	6.70108	3.86500	17.40581
O	3.422	3.56906	17.53884
O	-0.07371	3.12549	17.24711
O	11.41843	10.88854	17.49281
O	9.18981	10.58636	17.52086
O	-0.10579	11.18342	17.21132
O	2.89618	11.00698	17.39423
O	5.87127	10.91659	17.48119
O	8.98629	8.37693	17.53089
O	1.13897	8.59441	17.44224
O	1.27127	5.60996	17.39977
O	12.093	8.52506	17.743
O	11.36203	6.16058	17.48423
O	6.33856	8.40836	17.53257
O	3.70895	8.51362	17.519
O	8.56861	6.16070	17.47570
O	6.35934	5.85169	17.519
O	3.54909	5.90796	17.53384

(Bottom)

Atom	X	Y	Z
Pd	0.00000	1.58807	7.00012
Pd	2.75064	1.58807	7.00012
Pd	5.50128	1.58807	7.00012
Pd	8.25192	1.58807	7.00012
Pd	11.00256	1.58807	7.00012
Pd	1.37532	3.97025	7.00012
Pd	4.12596	3.97025	7.00012
Pd	6.87660	3.97025	7.00012
Pd	9.62724	3.97025	7.00012
Pd	12.37788	3.97025	7.00012
Pd	0.00000	6.35229	7.00012
Pd	2.75064	6.35229	7.00012
Pd	5.50128	6.35229	7.00012
Pd	8.25192	6.35229	7.00012
Pd	11.00256	6.35229	7.00012
Pd	1.37532	8.73447	7.00012
Pd	4.12596	8.73447	7.00012
Pd	6.87660	8.73447	7.00012
Pd	9.62724	8.73447	7.00012
Pd	12.37788	8.73447	7.00012
Pd	0.00000	11.11665	7.00012
Pd	2.75064	11.11665	7.00012
Pd	5.50128	11.11665	7.00012
Pd	8.25192	11.11665	7.00012
Pd	11.00256	11.11665	7.00012
Pd	1.37532	2.38218	9.24584
Pd	4.12596	2.38218	9.24584
Pd	6.87660	2.38218	9.24584
Pd	9.62724	2.38218	9.24584
Pd	12.37788	2.38218	9.24584
Pd	0.00000	4.76422	9.24584
Pd	2.75064	4.76422	9.24584
Pd	5.50128	4.76422	9.24584
Pd	8.25192	4.76422	9.24584
Pd	11.00256	4.76422	9.24584
Pd	1.37532	7.140	9.24584
Pd	4.12596	7.140	9.24584
Pd	6.87660	7.140	9.24584
Pd	9.62724	7.140	9.24584
Pd	12.37788	7.140	9.24584
Pd	0.00000	9.52858	9.24584
Pd	2.75064	9.52858	9.24584
Pd	5.50128	9.52858	9.24584
Pd	8.25192	9.52858	9.24584
Pd	11.00256	9.52858	9.24584
Pd	1.37532	11.91062	9.24584
Pd	4.12596	11.91062	9.24584
Pd	6.87660	11.91062	9.24584

Pd	9.62724	11.91062	9.24584
Pd	12.37788	11.91062	9.24584
Pd	1.37532	0.79411	11.49180
Pd	4.12596	0.79411	11.49180
Pd	6.87660	0.79411	11.49180
Pd	9.62724	0.79411	11.49180
Pd	12.37788	0.79411	11.49180
Pd	0.00000	3.17615	11.49180
Pd	2.75064	3.17615	11.49180
Pd	5.50128	3.17615	11.49180
Pd	8.25192	3.17615	11.49180
Pd	11.00256	3.17615	11.49180
Pd	1.37532	5.55833	11.49180
Pd	4.12596	5.55833	11.49180
Pd	6.87660	5.55833	11.49180
Pd	9.62724	5.55833	11.49180
Pd	12.37788	5.55833	11.49180
Pd	0.00000	7.94051	11.49180
Pd	2.75064	7.94051	11.49180
Pd	5.50128	7.94051	11.49180
Pd	8.25192	7.94051	11.49180
Pd	11.00256	7.94051	11.49180
Pd	1.37532	10.32255	11.49180
Pd	4.12596	10.32255	11.49180
Pd	6.87660	10.32255	11.49180
Pd	9.62724	10.32255	11.49180
Pd	12.37788	10.32255	11.49180
Pd	0.00000	1.58807	13.73776
Pd	2.75064	1.58807	13.73776
Pd	5.50128	1.58807	13.73776
Pd	8.25192	1.58807	13.73776
Pd	11.00256	1.58807	13.73776
Pd	1.37532	3.97025	13.73776
Pd	4.12596	3.97025	13.73776
Pd	6.87660	3.97025	13.73776
Pd	9.62724	3.97025	13.73776
Pd	12.37788	3.97025	13.73776
Pd	0.00000	6.35229	13.73776
Pd	2.75064	6.35229	13.73776
Pd	5.50128	6.35229	13.73776
Pd	8.25192	6.35229	13.73776
Pd	11.00256	6.35229	13.73776
Pd	1.37532	8.73447	13.73776
Pd	4.12596	8.73447	13.73776
Pd	6.87660	8.73447	13.73776
Pd	9.62724	8.73447	13.73776
Pd	12.37788	8.73447	13.73776
Pd	0.00000	11.11665	13.73776
Pd	2.75064	11.11665	13.73776
Pd	5.50128	11.11665	13.73776
Pd	8.25192	11.11665	13.73776

Pd	11.00256	11.11665	13.73776

Pd Surface oxide (DFT optimized structures)
Top most atomic layer

Atom	X	Y	Z
Pd	7.95626000	4.35608000	17.57315000
Pd	5.20626000	12.60608000	17.57315000
Pd	2.45626000	7.10608000	17.57315000
Pd	-0.29374000	1.60608000	17.57315000
Pd	10.70626000	9.85608000	17.57315000
Pd	6.63901000	1.61161000	17.53525000
Pd	12.13901000	12.61161000	17.53525000
Pd	9.38901000	7.11161000	17.53525000
Pd	3.88901000	9.86161000	17.53525000
Pd	1.13901000	4.36161000	17.53525000
Pd	0.32432000	9.91044000	17.71125000
Pd	4.42562000	4.41688000	17.71029000
Pd	8.57432000	12.66044000	17.71125000
Pd	1.67562000	12.66688000	17.71029000
Pd	7.17562000	9.91688000	17.71029000
Pd	5.82432000	7.16044000	17.71125000
Pd	12.67562000	7.16688000	17.71029000
Pd	11.32432000	4.41044000	17.71125000
Pd	3.07432000	1.66044000	17.71125000
Pd	9.92562000	1.66688000	17.71029000
O	4.08119000	6.32531000	18.30337000
O	9.58119000	3.57531000	18.30337000
O	12.33119000	9.07531000	18.30337000
O	1.33119000	0.82531000	18.30337000
O	6.83119000	11.82531000	18.30337000
O	10.97229000	6.29067000	18.29681000
O	5.47229000	9.04067000	18.29681000
O	8.22229000	0.79067000	18.29681000
O	2.72229000	3.54067000	18.29681000
O	-0.02771000	11.79067000	18.29681000
O	7.63415000	7.99984000	17.17593000
O	4.88415000	2.49984000	17.17593000
O	10.38415000	-0.25016000	17.17593000
O	2.13415000	10.74984000	17.17593000
O	13.13415000	5.24984000	17.17593000
O	6.20209000	5.22891000	17.16574000
O	0.70209000	7.97891000	17.16574000
O	3.45209000	-0.27109000	17.16574000
O	11.70209000	2.47891000	17.16574000
O	8.95209000	10.72891000	17.16574000

(Bottom)

Atom	X	Y	Z
Pd	11.00000000	11.00000000	11.21000000
Pd	8.25000000	11.00000000	11.21000000
Pd	5.50000000	11.00000000	11.21000000
Pd	2.75000000	11.00000000	11.21000000
Pd	0.00000000	11.00000000	11.21000000
Pd	11.00000000	8.25000000	11.21000000
Pd	8.25000000	8.25000000	11.21000000
Pd	5.50000000	8.25000000	11.21000000
Pd	2.75000000	8.25000000	11.21000000
Pd	0.00000000	8.25000000	11.21000000
Pd	11.00000000	5.50000000	11.21000000
Pd	8.25000000	5.50000000	11.21000000
Pd	5.50000000	5.50000000	11.21000000
Pd	2.75000000	5.50000000	11.21000000
Pd	0.00000000	5.50000000	11.21000000
Pd	11.00000000	2.75000000	11.21000000
Pd	8.25000000	2.75000000	11.21000000
Pd	5.50000000	2.75000000	11.21000000
Pd	2.75000000	2.75000000	11.21000000
Pd	0.00000000	2.75000000	11.21000000
Pd	11.00000000	0.00000000	11.21000000
Pd	8.25000000	0.00000000	11.21000000
Pd	5.50000000	0.00000000	11.21000000
Pd	2.75000000	0.00000000	11.21000000
Pd	0.00000000	0.00000000	11.21000000
Pd	12.36893000	12.38903000	13.16985000
Pd	9.61929000	12.38326000	13.17261000
Pd	6.88628000	12.35333000	13.20810000
Pd	4.12703000	12.36266000	13.22370000
Pd	1.37742000	12.39370000	13.20266000
Pd	12.38628000	9.60333000	13.20810000
Pd	9.62703000	9.61266000	13.22370000
Pd	6.87742000	9.64370000	13.20266000
Pd	4.11893000	9.63903000	13.16985000
Pd	1.36929000	9.63326000	13.17261000
Pd	12.37742000	6.89370000	13.20266000
Pd	9.61893000	6.88903000	13.16985000
Pd	6.86929000	6.88326000	13.17261000
Pd	4.13628000	6.85333000	13.20810000
Pd	1.37703000	6.86266000	13.22370000
Pd	12.36929000	4.13326000	13.17261000
Pd	9.63628000	4.10333000	13.20810000
Pd	6.87703000	4.11266000	13.22370000
Pd	4.12742000	4.14370000	13.20266000
Pd	1.36893000	4.13903000	13.16985000
Pd	12.37703000	1.36266000	13.22370000
Pd	9.62742000	1.39370000	13.20266000
Pd	6.86893000	1.38903000	13.16985000

Pd	4.11929000	1.38326000	13.17261000
Pd	1.38628000	1.35333000	13.20810000
Pd	11.06404000	11.01525000	15.17333000
Pd	8.27789000	11.05304000	15.20473000
Pd	5.50737000	11.00994000	15.28967000
Pd	2.73066000	10.98538000	15.19231000
Pd	-0.089000	11.06475000	15.16055000
Pd	11.00737000	8.25994000	15.28967000
Pd	8.23066000	8.23538000	15.19231000
Pd	5.45311000	8.31475000	15.16055000
Pd	2.81404000	8.26525000	15.17333000
Pd	0.02789000	8.30304000	15.20473000
Pd	10.95311000	5.56475000	15.16055000
Pd	8.31404000	5.51525000	15.17333000
Pd	5.52789000	5.55304000	15.20473000
Pd	2.75737000	5.50994000	15.28967000
Pd	-0.01934000	5.48538000	15.19231000
Pd	11.02789000	2.80304000	15.20473000
Pd	8.25737000	2.75994000	15.28967000
Pd	5.48066000	2.73538000	15.19231000
Pd	2.70311000	2.81475000	15.16055000
Pd	0.06404000	2.76525000	15.17333000
Pd	10.98066000	-0.012000	15.19231000
Pd	8.20311000	0.06475000	15.16055000
Pd	5.56404000	0.01525000	15.17333000
Pd	2.77789000	0.05304000	15.20473000
Pd	0.00737000	0.00994000	15.28967000

Pd 2CO; 2OH; 5C_3H_6

Atom	X	Y	Z
Pd	12.3778800000	11.9106190240	15.9834849480
Pd	9.6272400000	11.9106190240	15.9834849480
Pd	6.8766000000	11.9106190240	15.9834849480
Pd	4.1259600000	11.9106190240	15.9834849480
Pd	1.3753200000	11.9106190240	15.9834849480
Pd	11.0025600000	9.5285809760	15.9834849480
Pd	8.2519200000	9.5285809760	15.9834849480
Pd	5.5012800000	9.5285809760	15.9834849480
Pd	2.7506400000	9.5285809760	15.9834849480
Pd	0.0000000000	9.5285809760	15.9834849480
Pd	12.3778800000	7.14000000	15.9834849480
Pd	9.6272400000	7.14000000	15.9834849480
Pd	6.8766000000	7.14000000	15.9834849480
Pd	4.1259600000	7.14000000	15.9834849480
Pd	1.3753200000	7.14000000	15.9834849480
Pd	11.0025600000	4.7642190240	15.9834849480
Pd	8.2519200000	4.7642190240	15.9834849480
Pd	5.5012800000	4.7642190240	15.9834849480
Pd	2.7506400000	4.7642190240	15.9834849480
Pd	0.0000000000	4.7642190240	15.9834849480
Pd	12.3778800000	2.3821809760	15.9834849480
Pd	9.6272400000	2.3821809760	15.9834849480
Pd	6.8766000000	2.3821809760	15.9834849480
Pd	4.1259600000	2.3821809760	15.9834849480
Pd	1.3753200000	2.3821809760	15.9834849480
Pd	11.0025600000	11.1166539840	13.7377573920
Pd	8.2519200000	11.1166539840	13.7377573920
Pd	5.5012800000	11.1166539840	13.7377573920
Pd	2.7506400000	11.1166539840	13.7377573920
Pd	0.0000000000	11.1166539840	13.7377573920
Pd	12.3778800000	8.7344730080	13.7377573920
Pd	9.6272400000	8.7344730080	13.7377573920
Pd	6.8766000000	8.7344730080	13.7377573920
Pd	4.1259600000	8.7344730080	13.7377573920
Pd	1.3753200000	8.7344730080	13.7377573920
Pd	11.0025600000	6.3522920320	13.7377573920
Pd	8.2519200000	6.3522920320	13.7377573920
Pd	5.5012800000	6.3522920320	13.7377573920
Pd	2.7506400000	6.3522920320	13.7377573920
Pd	0.0000000000	6.3522920320	13.7377573920
Pd	12.3778800000	3.9702539840	13.7377573920
Pd	9.6272400000	3.9702539840	13.7377573920
Pd	6.8766000000	3.9702539840	13.7377573920
Pd	4.1259600000	3.9702539840	13.7377573920
Pd	1.3753200000	3.9702539840	13.7377573920
Pd	11.0025600000	1.5880730080	13.7377573920
Pd	8.2519200000	1.5880730080	13.7377573920
Pd	5.5012800000	1.5880730080	13.7377573920
Pd	2.7506400000	1.5880730080	13.7377573920

Pd	0.0000000000	1.5880730080	13.7377573920
Pd	12.3778800000	10.32250160	11.4918000000
Pd	9.6272400000	10.32250160	11.4918000000
Pd	6.8766000000	10.32250160	11.4918000000
Pd	4.1259600000	10.32250160	11.4918000000
Pd	1.3753200000	10.32250160	11.4918000000
Pd	11.0025600000	7.9405079680	11.4918000000
Pd	8.2519200000	7.9405079680	11.4918000000
Pd	5.5012800000	7.9405079680	11.4918000000
Pd	2.7506400000	7.9405079680	11.4918000000
Pd	0.0000000000	7.9405079680	11.4918000000
Pd	12.3778800000	5.5583269920	11.4918000000
Pd	9.6272400000	5.5583269920	11.4918000000
Pd	6.8766000000	5.5583269920	11.4918000000
Pd	4.1259600000	5.5583269920	11.4918000000
Pd	1.3753200000	5.5583269920	11.4918000000
Pd	11.0025600000	3.17610160	11.4918000000
Pd	8.2519200000	3.17610160	11.4918000000
Pd	5.5012800000	3.17610160	11.4918000000
Pd	2.7506400000	3.17610160	11.4918000000
Pd	0.0000000000	3.17610160	11.4918000000
Pd	12.3778800000	0.7941079680	11.4918000000
Pd	9.6272400000	0.7941079680	11.4918000000
Pd	6.8766000000	0.7941079680	11.4918000000
Pd	4.1259600000	0.7941079680	11.4918000000
Pd	1.3753200000	0.7941079680	11.4918000000
Pd	12.3778800000	11.9106190240	9.2458426080
Pd	9.6272400000	11.9106190240	9.2458426080
Pd	6.8766000000	11.9106190240	9.2458426080
Pd	4.1259600000	11.9106190240	9.2458426080
Pd	1.3753200000	11.9106190240	9.2458426080
Pd	11.0025600000	9.5285809760	9.2458426080
Pd	8.2519200000	9.5285809760	9.2458426080
Pd	5.5012800000	9.5285809760	9.2458426080
Pd	2.7506400000	9.5285809760	9.2458426080
Pd	0.0000000000	9.5285809760	9.2458426080
Pd	12.3778800000	7.14000000	9.2458426080
Pd	9.6272400000	7.14000000	9.2458426080
Pd	6.8766000000	7.14000000	9.2458426080
Pd	4.1259600000	7.14000000	9.2458426080
Pd	1.3753200000	7.14000000	9.2458426080
Pd	11.0025600000	4.7642190240	9.2458426080
Pd	8.2519200000	4.7642190240	9.2458426080
Pd	5.5012800000	4.7642190240	9.2458426080
Pd	2.7506400000	4.7642190240	9.2458426080
Pd	0.0000000000	4.7642190240	9.2458426080
Pd	12.3778800000	2.3821809760	9.2458426080
Pd	9.6272400000	2.3821809760	9.2458426080
Pd	6.8766000000	2.3821809760	9.2458426080
Pd	4.1259600000	2.3821809760	9.2458426080
Pd	1.3753200000	2.3821809760	9.2458426080

Pd	11.0025600000	11.1166539840	7.0001150520
Pd	8.2519200000	11.1166539840	7.0001150520
Pd	5.5012800000	11.1166539840	7.0001150520
Pd	2.7506400000	11.1166539840	7.0001150520
Pd	0.0000000000	11.1166539840	7.0001150520
Pd	12.3778800000	8.7344730080	7.0001150520
Pd	9.6272400000	8.7344730080	7.0001150520
Pd	6.8766000000	8.7344730080	7.0001150520
Pd	4.1259600000	8.7344730080	7.0001150520
Pd	1.3753200000	8.7344730080	7.0001150520
Pd	11.0025600000	6.3522920320	7.0001150520
Pd	8.2519200000	6.3522920320	7.0001150520
Pd	5.5012800000	6.3522920320	7.0001150520
Pd	2.7506400000	6.3522920320	7.0001150520
Pd	0.0000000000	6.3522920320	7.0001150520
Pd	12.3778800000	3.9702539840	7.0001150520
Pd	9.6272400000	3.9702539840	7.0001150520
Pd	6.8766000000	3.9702539840	7.0001150520
Pd	4.1259600000	3.9702539840	7.0001150520
Pd	1.3753200000	3.9702539840	7.0001150520
Pd	11.0025600000	1.5880730080	7.0001150520
Pd	8.2519200000	1.5880730080	7.0001150520
Pd	5.5012800000	1.5880730080	7.0001150520
Pd	2.7506400000	1.5880730080	7.0001150520
Pd	0.0000000000	1.5880730080	7.0001150520
O	2.59303	7.23131	18.87082
O	4.00350	2.55399	17.99488
O	11.86360	7.74100	19.03870
O	11.716	2.57131	17.87944
C	2.51423	7.19801	17.81722
C	13.04997	12.99258	17.71114
C	12.45757	11.89568	18.44294
C	11.91137	12.00028	19.65994
C	8.79001	4.83944	18.06384
C	8.19761	3.74254	18.79564
C	7.65141	3.84714	20.01264
C	6.23169	9.76363	17.99030
C	5.63929	8.66675	18.72215
C	5.09311	8.77138	19.93913
C	1.77302	12.90098	17.85120
C	1.18062	11.80408	18.58300
C	0.71485	2.743	18.00142
C	0.63442	11.90868	19.80000
C	0.12245	1.64953	18.73322
C	-0.42375	1.75413	19.95022
C	11.78489	7.70771	17.98512
H	3.86770	2.70279	18.94378
H	11.58071	2.72012	18.82830
H	14.09647	12.76638	17.50044
H	13.01347	13.94218	18.25044
H	12.45877	11.00158	18.00594

H	11.88247	12.86688	20.14264
H	11.52047	11.20668	20.10894
H	9.83651	4.61324	17.85314
H	8.75351	5.78904	18.60314
H	8.19881	2.84844	18.35864
H	7.62251	4.71374	20.49534
H	7.27827	9.53745	17.77962
H	7.26051	3.05354	20.164
H	6.19522	10.71324	18.52960
H	5.64052	7.77265	18.28507
H	5.06424	9.63790	20.42182
H	4.70219	7.97778	20.38815
H	2.81952	12.67478	17.64050
H	1.76135	2.52023	17.79072
H	1.73652	13.85058	18.39050
H	1.18182	10.90998	18.100
H	0.67835	3.69603	18.54072
H	0.60552	12.77528	20.28270
H	0.24352	11.11508	20.24900
H	0.12365	0.75543	18.29622
H	-0.45265	2.62073	20.43292
H	-0.815	0.96053	20.39922

PdO

Atom	X	Y	Z
Pd	0.000000	1.515000	2.665000
Pd	0.000000	1.515000	7.995000
Pd	0.000000	1.515000	13.325000
Pd	0.000000	4.545000	2.665000
Pd	0.000000	4.545000	7.995000
Pd	0.000000	4.545000	13.325000
Pd	0.000000	7.575000	2.665000
Pd	0.000000	7.575000	7.995000
Pd	0.000000	7.575000	13.325000
Pd	0.000000	10.605000	2.665000
Pd	0.000000	10.605000	7.995000
Pd	0.000000	10.605000	13.325000
Pd	3.030000	1.515000	2.665000
Pd	3.030000	1.515000	7.995000
Pd	3.030000	1.515000	13.325000
Pd	3.030000	4.545000	2.665000
Pd	3.030000	4.545000	7.995000
Pd	3.030000	4.545000	13.325000
Pd	3.030000	7.575000	2.665000
Pd	3.030000	7.575000	7.995000
Pd	3.030000	7.575000	13.325000
Pd	3.030000	10.605000	2.665000
Pd	3.030000	10.605000	7.995000
Pd	3.030000	10.605000	13.325000
Pd	6.060000	1.515000	2.665000
Pd	6.060000	1.515000	7.995000
Pd	6.060000	1.515000	13.325000
Pd	6.060000	4.545000	2.665000
Pd	6.060000	4.545000	7.995000
Pd	6.060000	4.545000	13.325000
Pd	6.060000	7.575000	2.665000
Pd	6.060000	7.575000	7.995000
Pd	6.060000	7.575000	13.325000
Pd	6.060000	10.605000	2.665000
Pd	6.060000	10.605000	7.995000
Pd	6.060000	10.605000	13.325000
Pd	9.090000	1.515000	2.665000
Pd	9.090000	1.515000	7.995000
Pd	9.090000	1.515000	13.325000
Pd	9.090000	4.545000	2.665000
Pd	9.090000	4.545000	7.995000
Pd	9.090000	4.545000	13.325000
Pd	9.090000	7.575000	2.665000
Pd	9.090000	7.575000	7.995000
Pd	9.090000	7.575000	13.325000
Pd	9.090000	10.605000	2.665000
Pd	9.090000	10.605000	7.995000
Pd	9.090000	10.605000	13.325000

Pd	1.515000	0.000000	0.000000
Pd	1.515000	0.000000	5.330000
Pd	1.515000	0.000000	10.660000
Pd	1.515000	0.000000	15.990000
Pd	1.515000	3.030000	0.000000
Pd	1.515000	3.030000	5.330000
Pd	1.515000	3.030000	10.660000
Pd	1.515000	3.030000	15.990000
Pd	1.515000	6.060000	0.000000
Pd	1.515000	6.060000	5.330000
Pd	1.515000	6.060000	10.660000
Pd	1.515000	6.060000	15.990000
Pd	1.515000	9.090000	0.000000
Pd	1.515000	9.090000	5.330000
Pd	1.515000	9.090000	10.660000
Pd	1.515000	9.090000	15.990000
Pd	1.515000	12.120000	0.000000
Pd	1.515000	12.120000	5.330000
Pd	1.515000	12.120000	10.660000
Pd	1.515000	12.120000	15.990000
Pd	4.545000	0.000000	0.000000
Pd	4.545000	0.000000	5.330000
Pd	4.545000	0.000000	10.660000
Pd	4.545000	0.000000	15.990000
Pd	4.545000	3.030000	0.000000
Pd	4.545000	3.030000	5.330000
Pd	4.545000	3.030000	10.660000
Pd	4.545000	3.030000	15.990000
Pd	4.545000	6.060000	0.000000
Pd	4.545000	6.060000	5.330000
Pd	4.545000	6.060000	10.660000
Pd	4.545000	6.060000	15.990000
Pd	4.545000	9.090000	0.000000
Pd	4.545000	9.090000	5.330000
Pd	4.545000	9.090000	10.660000
Pd	4.545000	9.090000	15.990000
Pd	4.545000	12.120000	0.000000
Pd	4.545000	12.120000	5.330000
Pd	4.545000	12.120000	10.660000
Pd	4.545000	12.120000	15.990000
Pd	7.575000	0.000000	0.000000
Pd	7.575000	0.000000	5.330000
Pd	7.575000	0.000000	10.660000
Pd	7.575000	0.000000	15.990000
Pd	7.575000	3.030000	0.000000
Pd	7.575000	3.030000	5.330000
Pd	7.575000	3.030000	10.660000
Pd	7.575000	3.030000	15.990000
Pd	7.575000	6.060000	0.000000
Pd	7.575000	6.060000	5.330000
Pd	7.575000	6.060000	10.660000

Pd	7.575000	6.060000	15.990000
Pd	7.575000	9.090000	0.000000
Pd	7.575000	9.090000	5.330000
Pd	7.575000	9.090000	10.660000
Pd	7.575000	9.090000	15.990000
Pd	7.575000	12.120000	0.000000
Pd	7.575000	12.120000	5.330000
Pd	7.575000	12.120000	10.660000
Pd	7.575000	12.120000	15.990000
O	0.000000	0.000000	1.332500
O	0.000000	0.000000	6.662500
O	0.000000	0.000000	11.992500
O	0.000000	3.030000	1.332500
O	0.000000	3.030000	6.662500
O	0.000000	3.030000	11.992500
O	0.000000	6.060000	1.332500
O	0.000000	6.060000	6.662500
O	0.000000	6.060000	11.992500
O	0.000000	9.090000	1.332500
O	0.000000	9.090000	6.662500
O	0.000000	9.090000	11.992500
O	0.000000	12.120000	1.332500
O	0.000000	12.120000	6.662500
O	0.000000	12.120000	11.992500
O	3.030000	0.000000	1.332500
O	3.030000	0.000000	6.662500
O	3.030000	0.000000	11.992500
O	3.030000	3.030000	1.332500
O	3.030000	3.030000	6.662500
O	3.030000	3.030000	11.992500
O	3.030000	6.060000	1.332500
O	3.030000	6.060000	6.662500
O	3.030000	6.060000	11.992500
O	3.030000	9.090000	1.332500
O	3.030000	9.090000	6.662500
O	3.030000	9.090000	11.992500
O	3.030000	12.120000	1.332500
O	3.030000	12.120000	6.662500
O	3.030000	12.120000	11.992500
O	6.060000	0.000000	1.332500
O	6.060000	0.000000	6.662500
O	6.060000	0.000000	11.992500
O	6.060000	3.030000	1.332500
O	6.060000	3.030000	6.662500
O	6.060000	3.030000	11.992500
O	6.060000	6.060000	1.332500
O	6.060000	6.060000	6.662500
O	6.060000	6.060000	11.992500
O	6.060000	9.090000	1.332500
O	6.060000	9.090000	6.662500
O	6.060000	9.090000	11.992500

O	6.060000	12.120000	1.332500
O	6.060000	12.120000	6.662500
O	6.060000	12.120000	11.992500
O	9.090000	0.000000	1.332500
O	9.090000	0.000000	6.662500
O	9.090000	0.000000	11.992500
O	9.090000	3.030000	1.332500
O	9.090000	3.030000	6.662500
O	9.090000	3.030000	11.992500
O	9.090000	6.060000	1.332500
O	9.090000	6.060000	6.662500
O	9.090000	6.060000	11.992500
O	9.090000	9.090000	1.332500
O	9.090000	9.090000	6.662500
O	9.090000	9.090000	11.992500
O	9.090000	12.120000	1.332500
O	9.090000	12.120000	6.662500
O	9.090000	12.120000	11.992500
O	0.000000	0.000000	3.997500
O	0.000000	0.000000	9.327499
O	0.000000	0.000000	14.657499
O	0.000000	3.030000	3.997500
O	0.000000	3.030000	9.327499
O	0.000000	3.030000	14.657499
O	0.000000	6.060000	3.997500
O	0.000000	6.060000	9.327499
O	0.000000	6.060000	14.657499
O	0.000000	9.090000	3.997500
O	0.000000	9.090000	9.327499
O	0.000000	9.090000	14.657499
O	0.000000	12.120000	3.997500
O	0.000000	12.120000	9.327499
O	0.000000	12.120000	14.657499
O	3.030000	0.000000	3.997500
O	3.030000	0.000000	9.327499
O	3.030000	0.000000	14.657499
O	3.030000	3.030000	3.997500
O	3.030000	3.030000	9.327499
O	3.030000	3.030000	14.657499
O	3.030000	6.060000	3.997500
O	3.030000	6.060000	9.327499
O	3.030000	6.060000	14.657499
O	3.030000	9.090000	3.997500
O	3.030000	9.090000	9.327499
O	3.030000	9.090000	14.657499
O	3.030000	12.120000	3.997500
O	3.030000	12.120000	9.327499
O	3.030000	12.120000	14.657499
O	6.060000	0.000000	3.997500
O	6.060000	0.000000	9.327499
O	6.060000	0.000000	14.657499

O	6.060000	3.030000	3.997500
O	6.060000	3.030000	9.327499
O	6.060000	3.030000	14.657499
O	6.060000	6.060000	3.997500
O	6.060000	6.060000	9.327499
O	6.060000	6.060000	14.657499
O	6.060000	9.090000	3.997500
O	6.060000	9.090000	9.327499
O	6.060000	9.090000	14.657499
O	6.060000	12.120000	3.997500
O	6.060000	12.120000	9.327499
O	6.060000	12.120000	14.657499
O	9.090000	0.000000	3.997500
O	9.090000	0.000000	9.327499
O	9.090000	0.000000	14.657499
O	9.090000	3.030000	3.997500
O	9.090000	3.030000	9.327499
O	9.090000	3.030000	14.657499
O	9.090000	6.060000	3.997500
O	9.090000	6.060000	9.327499
O	9.090000	6.060000	14.657499
O	9.090000	9.090000	3.997500
O	9.090000	9.090000	9.327499
O	9.090000	9.090000	14.657499
O	9.090000	12.120000	3.997500
O	9.090000	12.120000	9.327499
O	9.090000	12.120000	14.657499
O	-0.000000	-0.000000	-1.332500
O	3.030000	-0.000000	-1.332500
O	0.000000	0.000000	17.322500
O	3.030000	0.000000	17.322500
O	0.000000	3.030000	-1.332500
O	3.030000	3.030000	-1.332500
O	0.000000	3.030000	17.322500
O	3.030000	3.030000	17.322500
O	0.000000	6.060000	-1.332500
O	3.030000	6.060000	-1.332500
O	0.000000	6.060000	17.322500
O	3.030000	6.060000	17.322500
O	0.000000	9.090000	-1.332500
O	3.030000	9.090000	-1.332500
O	0.000000	9.090000	17.322500
O	3.030000	9.090000	17.322500
O	0.000000	12.120000	-1.332500
O	3.030000	12.120000	-1.332500
O	0.000000	12.120000	17.322500
O	3.030000	12.120000	17.322500
O	6.060000	-0.000000	-1.332500
O	6.060000	0.000000	17.322500
O	6.060000	3.030000	-1.332500
O	6.060000	3.030000	17.322500

O	6.060000	6.060000	-1.332500
O	6.060000	6.060000	17.322500
O	6.060000	9.090000	-1.332500
O	6.060000	9.090000	17.322500
O	6.060000	12.120000	-1.332500
O	6.060000	12.120000	17.322500
O	9.090000	-0.000000	-1.332500
O	9.090000	0.000000	17.322500
O	9.090000	3.030000	-1.332500
O	9.090000	3.030000	17.322500
O	9.090000	6.060000	-1.332500
O	9.090000	6.060000	17.322500
O	9.090000	9.090000	-1.332500
O	9.090000	9.090000	17.322500
O	9.090000	12.120000	-1.332500
O	9.090000	12.120000	17.322500

References

1 P. Amann, D. Degerman, M.-T. Lee, J. D. Alexander, M. Shipilin, H.-Y. Wang, F. Cavalca, M. Weston, J. Gladh, M. Blom, M. Björkhage, P. Löfgren, C. Schlueter, P. Loemker, K. Ederer, W. Drube, H. Noei, J. Zehetner, H. Wentzel, J. Åhlund and A. Nilsson, *Rev. Sci. Instrum.*, 2019, **90**, 103102.

2 M. Brun, A. Berthet and J. . Bertolini, *J. Electron Spectros. Relat. Phenomena*, 1999, **104**, 55–60.

3 A. E. Bolzán, M. E. Martins and A. J. Arvía, *J. Electroanal. Chem. Interfacial Electrochem.*, 1984, **172**, 221–233.

4 A. Bolzan, M. E. Martins and A. J. Arvia, *J. Electroanal. Chem. Interfacial Electrochem.*, 1986, **207**, 279–292.

5 A. Winiwarter, L. Silvioli, S. B. Scott, K. Enemark-Rasmussen, M. Sariç, D. B. Trimarco, P. C. K. Vesborg, P. G. Moses, I. E. L. Stephens, B. Seger, J. Rossmeisl and I. Chorkendorff, *Energy Environ. Sci.*, 2019, **12**, 1055–1067.

6 D. Friebel, V. Viswanathan, D. J. Miller, T. Anniyev, H. Ogasawara, A. H. Larsen, C. P. Ogrady, J. K. Nørskov and A. Nilsson, *J. Am. Chem. Soc.*, 2012, **134**, 9664–9671.

7 L. Vitos, A. V. Ruban, H. L. Skriver and J. Kollár, *Surf. Sci.*, 1998, **411**, 186–202.

8 J. H. Stenlid, E. C. Dos Santos, A. Bagger, A. J. Johansson, J. Rossmeisl and L. G. M. Pettersson, *J. Phys. Chem. C*, 2020, **124**, 469–481.

9 J. H. Stenlid, E. Campos dos Santos, R. M. Arán Ais, A. Bagger, A. J. Johansson, B. R. Cuenya, J. Rossmeisl and L. G. M. Pettersson, *Electrochim. Acta*, 2020, 137111.

10 S. Grimme, J. Antony, S. Ehrlich and H. Krieg, *J. Chem. Phys.*, 2010, **132**, 154104.

11 S. Grimme, S. Ehrlich and L. Goerigk, *J. Comput. Chem.*, 2011, **32**, 1456–1465.

12 J. P. Perdew, K. Burke and M. Ernzerhof, *Phys. Rev. Lett.*, 1996, **77**, 3865–3868.

13 G. Kresse and J. Furthmüller, *Phys. Rev. B*, 1996, **54**, 11169–11186.

14 J. H. Stenlid, M. Soldemo, A. J. Johansson, C. Leygraf, M. Göthelid, J. Weissenrieder and T. Brinck, *Phys. Chem. Chem. Phys.*, 2016, **18**, 30570–30584.

15 L. Bengtsson, *Phys. Rev. B*, 1999, **59**, 12301–12304.

16 J. K. Nørskov, J. Rossmeisl, A. Logadottir, L. Lindqvist, J. R. Kitchin, T. Bligaard and H. Jónsson, *J. Phys. Chem. B*, 2004, **108**, 17886–17892.

17 S. Trasatti, *Pure Appl. Chem.*, **58**, 955–966.

18 J. Rossmeisl, K. Chan, R. Ahmed, V. Tripković and M. E. Björketun, *Phys. Chem. Chem. Phys.*, 2013, **15**, 10321–10325.

19 T. Allison, 1996.

20 J. D' Ans and E. Lax, *Taschenbuch für Chemiker und Physiker*, Springer-Verlag, 1983.

21 P. E. Blöchl, *Phys. Rev. B*, 1994, **50**, 17953–17979.

22 G. Kresse and D. Joubert, *Phys. Rev. B*, 1999, **59**, 1758–1775.

23 M. Methfessel and A. T. Paxton, *Phys. Rev. B*, 1989, **40**, 3616–3621.

24 A. Bagger, R. M. Arán-Ais, J. Halldin Stenlid, E. Campos dos Santos, L. Arnarson, K. Degn Jensen, M. Escudero-Escribano, B. Roldan Cuenya and J. Rossmeisl, *ChemPhysChem*, 2019, **20**, 3096–3105.

25 J. J. Rehr, J. J. Kas, F. D. Vila, M. P. Prange and K. Jorissen, *Phys. Chem. Chem. Phys.*, 2010, **12**, 5503–5513.

26 D. Friebel, D. J. Miller, C. P. O'Grady, T. Anniyev, J. Bargar, U. Bergmann, H. Ogasawara, K. T. Wikfeldt, L. G. M. Pettersson and A. Nilsson, *Phys. Chem. Chem. Phys.*, 2011, **13**, 262–266.

27 D. Friebel, D. J. Miller, D. Nordlund, H. Ogasawara and A. Nilsson, *Angew. Chemie - Int. Ed.*, 2011, **50**, 10190–10192.

28 A. Jain, S. P. Ong, G. Hautier, W. Chen, W. D. Richards, S. Dacek, S. Cholia, D. Gunter, D. Skinner, G. Ceder and K. A. Persson, *APL Mater.*, 2013, **1**, 11002.

29 J. Gustafson, M. Shipilin, C. Zhang, A. Stierle, U. Hejral, U. Ruett, O. Gutowski, P.-A. Carlsson, M. Skoglundh and E. Lundgren, *Science (80-.).*, 2014, **343**, 758–761.